UNIVERSITY OF PARMA

PhD in Biotechnology

(XXVIII cycle)

Competitive amperometric immunosensor for determination of p53 protein in urine: a rapid and noninvasive screening tool for early diagnosis of bladder carcinoma

PhD Coordinator:
Prof. Nelson Marmiroli

PhD Tutors:
Dr. Marco Giannetto
Dr.ssa Roberta Ruotolo
Prof.ssa Elena Maestri

PhD Student: Maria Vittoria Bianchi

Contents

Introduction

1. The Tumor Suppressor p53: cancer implications

1.1 Tumor suppressor genes: the brake of cell growth

Carcinogenesis is the process by which a normal cell becomes malignant, or becomes able to grow in an uncontrolled and disorganized way, invading surrounding tissues.

A cell becomes cancerous when the control mechanisms that regulate the cell cycle are modified in some way, with occourence of mutations that affect genes involved in the activation of the cell cycle (oncogenes), or mutations affecting genes that suppress the duplication of the cell (oncosuppressor genes).

Oncogenes are the first to be related with cancer. Genetic changes in these sites may give rise to cells unable to regulate their proliferative activity in response to inhibitor stimuli on the growth. Cells with mutations in one or more oncogenes may therefore be capable of proliferating in a complete uncontrolled way, thus giving origin to a neoplastic tissue.

In recent years it was discovered a remarkably different class of cancer-related genes: **tumor suppressor genes**. They do not act in normal cells by promoting cell proliferation, but suppressing them. Their inactivation, due to genetic alterations, results in the loss of the normal mechanisms of "brake" of cell growth and allows the cell, that carriers the tumor suppressor genes, to transform itself into cancer cell.

Research on tumor suppressor genes is currently very intense. Mutations in this gene sites have been found in a large variety of human tumors: it seems increasingly founded the hypothesis that these are own the most important genetic alterations in carcinogenesis.

A fundamental characteristic, in addition to the different function on the cell cycle, distinguishes oncogenes respect tumor suppressor genes. The oncogenes studied to date are always activated through somatic mutations, i.e. genetic alterations that occur in any cell of the body but that can not occur in germ cells. Activated mutated oncogenes are therefore not usually transmitted from parent to offspring.

Conversely, mutant forms of suppressor genes of growth can actually be found in germ cells (sperm or egg cells) and may therefore be transmitted from generation to generation. Obviously, a child who, at the time of conception, inherits a mutated tumor suppressor gene and is therefore heterozygous for a germline mutation will have a higher chance of developing cancer later in life[1].

At the basis of the majority of hereditary tumors there is, in effect, a state of heterozygosity for a

tumor suppressor gene.

1.2 p53: a “guardian of the genome”

15 years after its identification, p53 is still considered the most important tumor suppressor.
“Guardian of the genome” (Lane, 1992), “Death star” (Vousden, 2000), “Good and bad cop” (Sharpless and DePinho, 2002), “An acrobat in tumorigenesis” (Moll and Schramm, 1998), are just a few of the names that have been attributed to the p53 gene over recent years.
In 1992, the "Time" magazine has assigned to this protein the second place among the scientific topics of greatest interest and in 1993 p53 was declared "Molecule of the Year" by the magazine "Science", one of the most respected scientific journals in the world[2,3].
p53, also known as tumor protein 53 (TP53), is an effective transcription factor, responding to diverse cellular stresses to regulate expression of target genes involved in different activities including cell cycle arrest, DNA repair, cell senescence or apoptosis, depending on the extent of cell damage and other factors not yet known[4]. The overall result of the functions of p53 is the inhibition of cell growth. Some gene mutations may result in p53 mutants that lose their normal inhibitory function on cell replication and acquire a new stimulatory activity on the cell growth.

1.2.1 The discovery of p53

The history of p53 is a chaotic voyage from the world of oncogenes to the world of tumour suppressor genes, while retaining a certain degree of individuality.
p53 was identified for the first time in 1979 (by DeLeo et al., Kress et al., Lane and Crawford, Linzer and Levine) in SV40-transformed cells as a cellular protein that form a complex with the large T antigen and for that classified as oncoprotein[5,6]. Since this protein seemed not share antigenic determinants with antigen "large T" of SV40 and since the protein was later isolated also from murine embryonic carcinoma cells not infected with SV40, it was concluded that p53 is instead encoded by a cellular gene, and not by a viral gene[7]. Subsequently it was demonstrated that the peptide sequence of p53 is highly conserved in different species of vertebrates and this indicated that the protein had to play an important role in cellular physiology. Subsequent studies have established that the p53 protein is present in small concentrations in normal cells, while this concentration is significantly much higher in both tumor cell lines grown *in vitro* and in tumor tissues *in vivo*[8-10]. The molecular basis of this increase of p53 levels in cancer cells is probably due to a stabilization of the post-transcriptional phenomenon, due to changes in the cellular environment, or to the formation of complexes with other cellular or viral proteins. The result is

anyhow an increase in the half-life time of the protein, which causes the accumulation of the same protein and therefore an increase in its concentration[8-10].

The majority of the mutations of the gene sequence coding for p53 have the same effect[5,6]. The observation that many transformed cells containing more p53 compared to corresponding normal cells indicates that this protein could play an important role in cell cycle control and that the increased expression of p53 would lead to an increase in cell proliferation, so it was thought that the p53 protein was the product of an oncogene[7]. Subsequent observations indicated that the p53 gene is able to cooperate with the oncogene ras in the transformation of rat embryo fibroblasts continuing to support the hypothesis that p53 was a dominant oncogene, and that it contributed to tumorigenesis by providing a stimulus for cell growth when it was overexpressed[6].

In 1989 Hind et al[11] have shown that, in fact, many of the studies in which the TP53 gene was co-transfected with the ras gene have been made with clones of mutant p53. When these experiments were repeated by co-transfection with cDNA of TP53 "wild type" (not alter), there was no transformation of fibroblasts. Therefore, these results have allowed to establish that TP53 is a tumor suppressor gene that normally inhibits cell growth; in certain cases some mutations affecting this gene can give rise to mutant p53 proteins which not only lose their normal function of "brake" on cell duplication but who also purchase a new oncogenic activity type, i.e. stimulatory towards the growth of the cell.

1.2.2 Structure of p53

The *TP53* gene is located on the short arm of human chromosome 17 at 17p13.1 position and consists of eleven exons (the first of which is non-coding)[12], for a total length of about 20 kb (Figure 1). The *TP53* gene is expressed in almost all tissues and is highly conserved in all vertebrate species.

The protein product of the *TP53* gene is a nuclear phosphoprotein formed by 393 amino acids (MW 53 KDa).

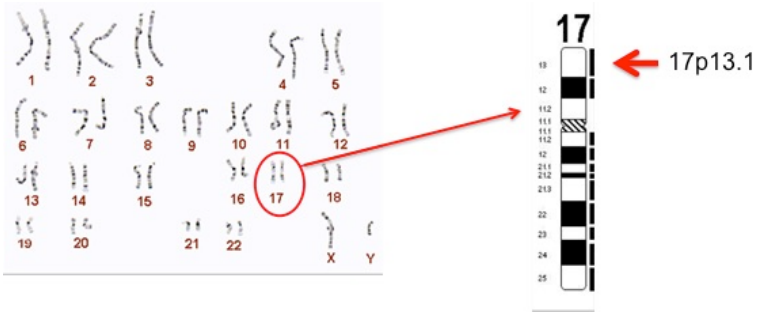

Figure 1: Localization of human gene *TP53*

The human p53 protein (Hp53) presents an acidic domain (residues 1-80), a hydrophobic domain (residues 75-150) and a basic domain (residues 319-393) and can be divided into five domains, each corresponding to specific functions (Figure 2).

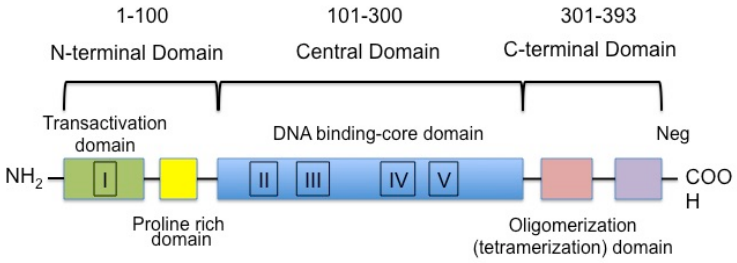

Figure 2: Structure of human p53 protein (Hp53)

1. The amino-terminus part (1 - 58) contains the acid transactivation domain (*transcription activation domain, TAD*), and the mdm2 protein binding site (protein that has inhibitory action on the transactivation process of p53)[13]. It also contains a highly conserved domain (HCD I).
2. The proline-rich domain (64 - 92, *PRD*) contains repeated series of proline residues that are conserved in the majority of p53. It also contains a second transactivation domain.
3. The central region (102 - 292) called core DNA-binding domain (*DBD*) allows the binding of the protein with the DNA of downstream genes[14]. It is the target of 90% of p53 mutations found in human cancer[15]. It also contains four other highly conserved domains (HCD II – V).
4. The oligomerization domain (316 – 356, *OD*) is formed by a beta-strand, followed by an alpha-helix, necessary for the formation of a tetramer of p53 (p53 is composed of a dimer of two dimer, 4D): the tetramerization of the protein greatly increases the in vivo activity. A nuclear export signal (NES) is localized in this oligomerization domain.
5. The carboxy-terminus part of p53 (363 – 393, *CTD*) contains three nuclear localization signals (*NLS*) and a non-specific DNA binding domain that binds to damaged DNA. These regions are also involved in the down-regulation of DNA binding on central domain.

1.2.3 Quaternary structures of p53

The tumor suppressor p53 is a tetrameric, multidomain transcription factor that plays, as already mentioned, a central role in the cell cycle and maintaining genomic integrity[16,17].

The intimate and multifaceted role of p53 in cell cycle is reflected in its equally complex biological structure that has been revealed slowly. The concerted action of the folded domains of the highly dynamic and intrinsically disordered p53, provides promiscuity and binding specificity, allowing it to process a multitude of cellular signals[18].

The human p53 protein is a flexible molecule biologically active as homo-tetramer composed of four identical polypeptide chains, each of which, as already said, it is constituted by 393 amino acids[19]. Each chain consists of two folded domains [the core, or DNA-binding, domain and the tetramerization domain] that are linked by an intrinsically disordered sequence (Figure 3)[20]. The transactivation domain, proline-rich region, nuclear localization signal (NLS)-containing region, and C-terminal negative regulatory domain are also intrinsically disordered.

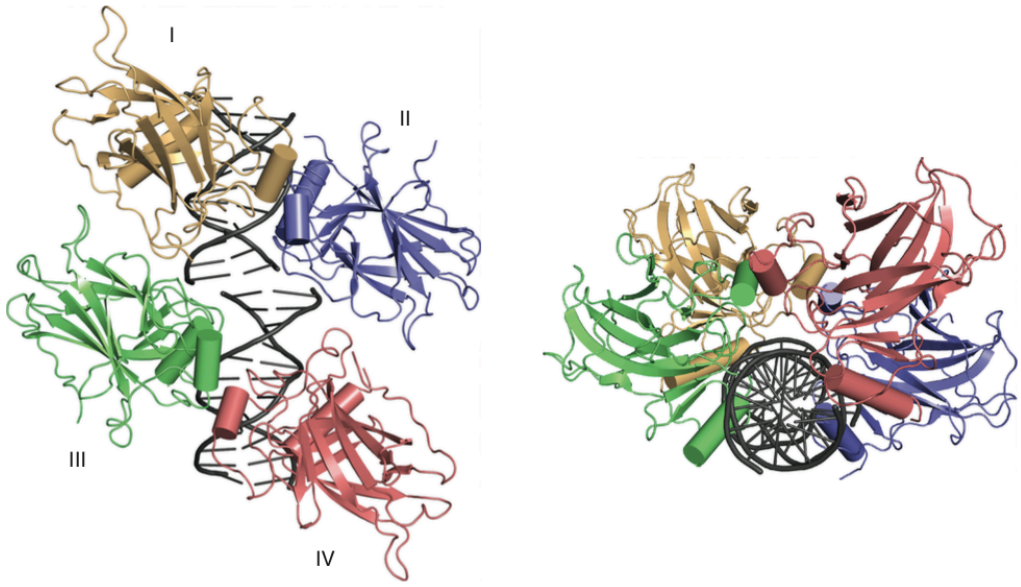

Figure 3: "Cartoon" Ribbon diagram of a core domain tetramer bound to DNA, with individual core domains depicted in different colors: representation of core domain-core domain contacts (*left*) and view along DNA helix axis (*right*)

Structural studies of the entire p53 were hampered both for its inherent instability, both for the presence of the disordered regions. It is also known that the flexible molecules are difficult to study with the X-ray crystallography because they do not form ordered crystals and even if they crystallize, the experimental images are often indistinct.

In 2007 Tidow and collaborators, through a multitechnique approach, are managed to determine the structure of tetrameric full-lenght human p53 (Figure 4), both unligated and as a complex with a DNA response element[21].

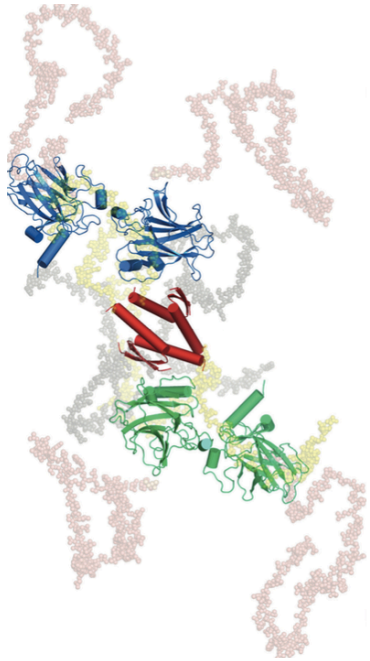

Figure 4: Models of full-length p53: in its unbound state. The p53 DNA-binding domains are shown in blue and green, the tetramerization domain in red.

1.2.4 Activation of p53 and cellular response

The p53 tumour suppressor is a tightly regulated protein that acts by stopping cell-cycle progression or promoting apoptosis when cells encounter stress stimuli. Since p53 has a short half-life (about 20-60 minutes), in unstressed mammalian cells is normally maintained at low levels by continuous ubiquitylation and subsequent degradation by the 26S proteasome. This is due to the interaction of p53 with the ubiquitin E3 ligase MDM2 protein. In normal cells, p53-MDM2 interaction involves a negative feed-back loop such that transcription of MDM2 (murine double minute 2) protein is stimulated by p53[22].

In stress conditions, post-translational modifications of p53 (most commonly phosphorylation of serine, less frequently acetylation of lysines), prevents binding of Mdm2 to p53[23,24] inducing the block of p53 ubiquitination. This results in the accumulation of p53 in the nucleus, where it forms a homotetrameric complex[25], and the activation of its gene transcription program that reflects the nature of the stress signal (environmental stress, DNA damage, activation of oncogenes, hypoxia)[26]. In this way is induced the expression of downstream genes that activate in their turn different paths of signal that can cause cell cycle arrest, apoptosis, DNA repair, differentiation, senescence[27]. p53 can also act outside of the nucleus to induce apoptosis by binding with anti-apoptotic proteins such as BCL2 (Figure 5).

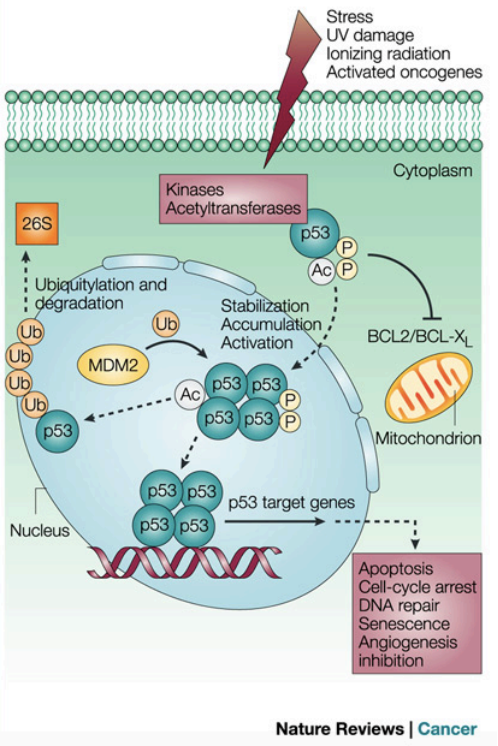

Figure 5: Activation of p53 and cellular response.

The p53 alterations caused by these external factors can affect the stability of the protein, the oligomerization, the DNA-binding and the binding to other proteins. p53 acts, therefore, as a sensor that integrates information from many paths, each of which leads to modification of specific residues of p53, activating its response. Normally, the phosphorylation of an aminoacid can change the properties of a protein by altering the structure in the immediate vicinity, creating or abolishing sites that interact with other proteins, but, in some of these sites of the p53, phosphorylation has a broader effect and changes the polypeptide conformation of the protein: it passes from a "trans" conformation (in which adjacent amino acids are located on opposite sides of the polypeptide bond) to a "cis" conformation (in which both the amino acids are located on the same side of the peptide bond). Therefore, the activation of p53 is determined by two factors: on the one hand the amount of p53 present in the cell (determined mainly from regulatory activity of mdm-2), and other changes of conformation caused by the action of one or more sensors systems as a result of environmental events[28].

1.2.5 TP53 mutations and cancer

The biological activity of p53 is closely related to the ability of the protein to bind to DNA and to act as a transcriptional factor.

The functional importance of the p53 DNA-binding domain (DBD) is demonstrated by the fact that over 70% of *TP53* mutations are missense mutations affecting residues within this domain (Figure 6) and lead to low capacity of target genes transactivation.

The most common mutations change the arginine 248 and arginine 273. Arg 248, in particular, is inserted in the minor groove of the DNA, forming a very stable interaction. The other most important sites of mutation, include residues of arginine 175, 249, 282, and glycine 245. Some of these come into direct contact with the DNA, while others maintain the correct position other amino acids that bind DNA. It is therefore clear that the change of only one of them is sufficient to produce the failure link between p53 and DNA and therefore the loss of p53 function.

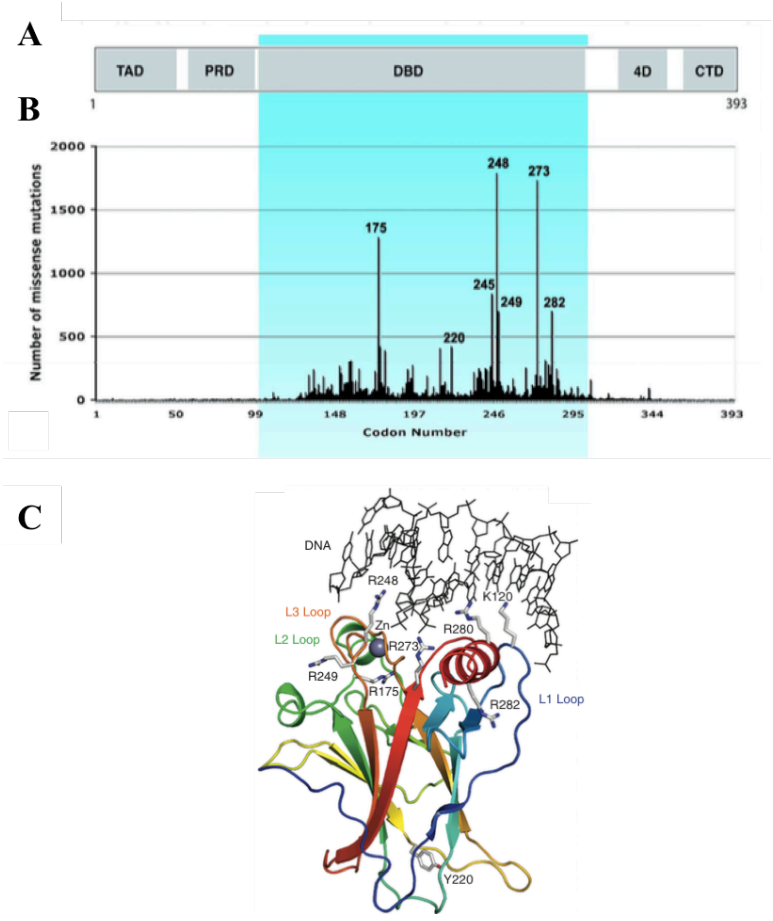

Figure 6: Missense mutations of *TP53* in the DNA binding domain (DBD). (A) Schematic representation of the p53 domains (B) The vertical bars indicate the relative missense-mutation frequency in human cancer for each residue (according to the IARC TP53 mutation database, R18), showing that most cancer mutations are located in the DNA-binding domain. (C) The structure of the DNA-binding domain, shown as stick models (PDB code 1TSR[29]), with indication of sites of cancer hotspot mutation and of essential DNA contacts.

The oligomerization of the p53 protein is also crucial for its tumor suppressor function[30].

Only tetrameric p53 seems to be fully active as a transcriptional activator or repressor of distinct

target genes that contain p53 sequence-specific DNA binding sites.

The conformation of the p53 protein is indeed closely related to its function: the p53 in the "wild-type" conformation is a repressor of cell growth, while some mutant forms of p53 have such a shape that gives them an activity promoter of cell duplication.

The crucial role of p53 in tumor suppression is demonstrated by the fact that the *TP53* gene is mutated in 50-70% of sporadic human cancers[31] and that genes encoding the p53 regulators, Mdm2 (Mouse Double Minute 2) and MDM4 (also known as MdmX), are often mutated in the remaining tumors[32]. Furthermore, germline mutations in one of the two alleles of p53, determine a high predisposition to the development of cancer; This is a familiar condition known as Li-Fraumeni syndrome[33].

More than 28.000 somatic mutations and close to 1.600 *TP53* germline mutations were reported according to the TP53 mutation database[34] of the International Agency for Research on Cancer (IARC, www-p53.iarc.fr), release R18, April 2016 (Figure 7 a,b). The loss of p53 function thus appears to be the most common alterations in human malignancies.

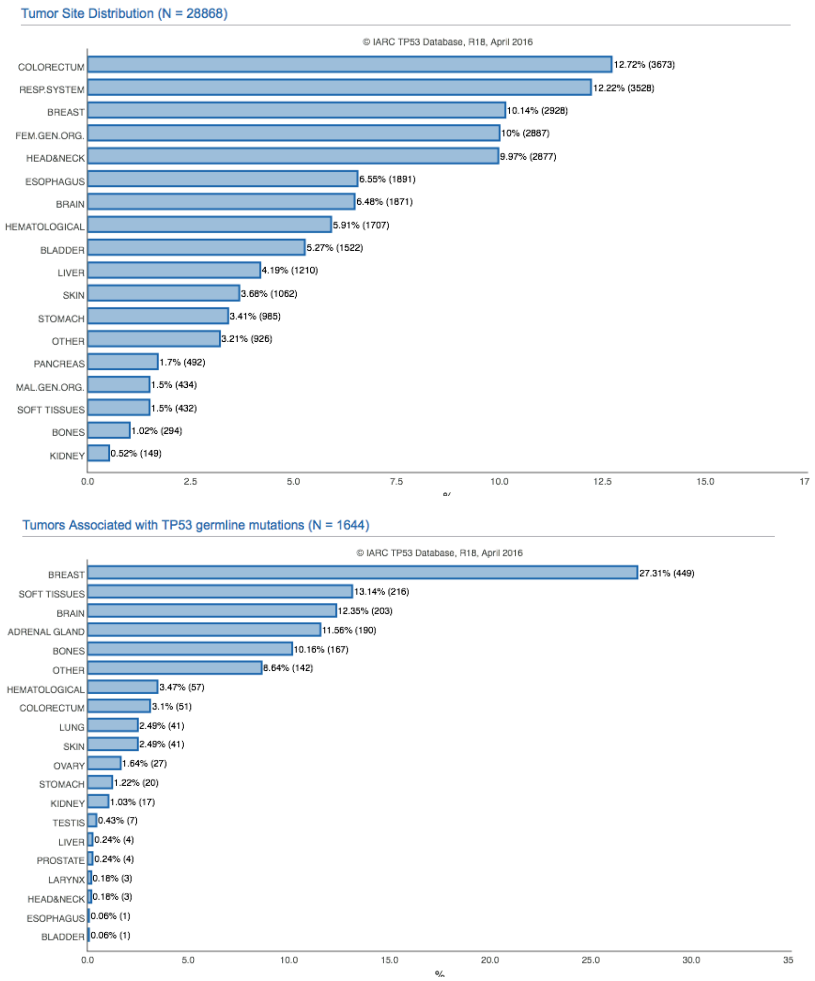

Figure 7: Cancers associated with *TP53* somatic and germline mutations, from IARC TP53 database, release R18, April 2016

TP53 mutations will accumulate in many types of human cancer that affect tissues and organs significantly different. The heterogeneity of the types of cancers indicates that the protein derived from this gene is not involved in a tissue-specific event, but in a common control mechanism of the cellular proliferation.

The half-life of a wild-type p53, as already mentioned, is short but with some mutations it increases and reaches up to 6 hours[6]. The mutated p53 protein prevents formation of the normal type of this protein due to the negative feedback caused by its long half-life[35]. This will result in the accumulation of the protein in the nucleus of the cell.

Given all these considerations is simple understand as p53 was currently considered a biomarker of crucial importance, specifically related to oncogenic disease. The presence of the wild-type or mutated form of p53 as well as its levels in can provide information valuable for clinical screening programs, for early cancer detection and for therapeutic purposes[36].

1.3 Role of p53 in Bladder Carcinoma

1.3.1 Bladder Transitional Cell Carcinoma (BTCC)

The term urothelium indicates the epithelium lining of the urinary tract that extends from the renal calyces to urethra (figure 8). This type of epithelium is transitional, consists of cells with polarity and architecturally organized layering to provide the best protection to an organ elastic and necessarily not permeable by its content. The urothelial lesions, which result from the pathological transformation of this particular epithelium, can be located in any point of the urinary tract and present a substantial uniformity as well as similar anatomical-clinical characters. Architecturally are divided into papillary and non-papillary tumors (Figure 8).

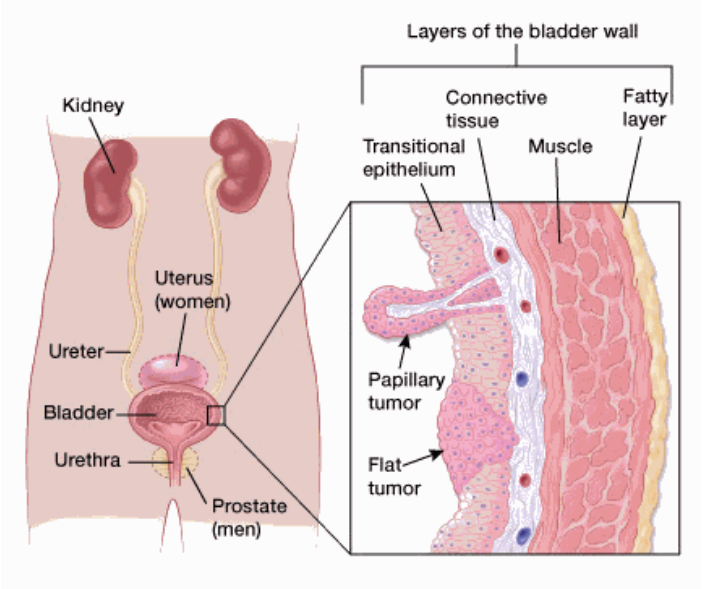

Figure 8: Front view of urinary tract (masculine and feminine) and layers of bladder wall.

Most of the 90% of urothelial neoplasia arises in the bladder, 8% originate in the renal pelvis and the remaining 2% originates in the ureter and urethra.

In most cases, bladder cancer starts in the transitional cells, i.e. the cells that make up its inner lining. The causes of this cancer are not completely understood, but there is a relationship with smoking, with urinary infections by parasites, with exposure to radiation or chemicals. The transitional cell carcinoma (TCC) represents more than 90% of bladder cancers, while squamous cell carcinomas and adenocarcinomas account for the remainder and is the fourth most cancer in men and the eighth in woman[37].

1.3.2 The correlation between mutated p53 protein and BTCC

Also for BTCC, the findings of molecular genetic studies evidenced the main role played by the mutations in the suppressor genes, responsible for the pathogenic mechanism of the malignancy and p53 is one of these suppressor genes. As already mentioned, the mutated p53 caracterized by a half-life increased, can prevent the formation of its wild-type form due to the onset of a negative feedback[35] with a consequent accumulation in the nucleus of the cell.

Furthermore, several clinical studies demonstrated that abnormal p53 protein accumulation in the epithelial cells may result in its overexpression at level of extracellular fluids, by an unknown mechanism, with particular relevance for urine[38-43]..

To support of what said, Darabi et al.[44] have shown that there is a highly association between a positive serum or urine sample for p53 protein and the overexpression of p53 protein in the tumoral tissue of patients with conclamate bladder TCC.

Therefore, p53 is a valuable protein biomarker associated to pathological and clinical parameters of the disease[37,45,46].

1.4 Analytical approaches for the determination of p53 protein

On the basis of the increasing clinical interest for the determination of p53 in cell lysates and biological fluids, a variety of analytical approaches, comprising matrix-assisted laser desorption/ionization time-of-flight mass spectrometry combined to high-performance liquid chromatography pre-fractioning[47], immunochemical methods[48,49] immunohistochemical methods[6] and surface-enhanced Raman spectroscopy[50] have been developed and proposed. Concerning the sensing devices, field effect transistors as well as surface plasmon resonators[51] have been investigated as biologically addressable substrates for the selective determination of p53.
These techniques require long run times and high costs, expecially if used for diagnostic. A valid alternative approach is represented by biosensor, which are faster, less expensive, compact and portable devices.

2. Immunosensors

2.1 Immunoassays: general principles

To date one of the most commonly used diagnostic analysis techniques for the determination of p53 in clinical samples involve an immunochemical approach, based on specific antibody-antigen interactions, as for the Enzyme-Linked Immuno-Sorbent Assay (ELISA) tests.
Immunoassays are tests used for the determination of antigens or antibodies, generally in serum samples, using respectively the antibody directed towards the antigen or the antigen to which the antibody is directed.
More specifically, these techniques are defined “enzyme immunoassays” (EIA) when, in addition to the specific antigen-antibody interaction, an enzymatic reaction for the production of an analytically measurable signal is also exploited.

2.1.1 ELISA assays

Among the most used immunochemical methods for the determination of antibodies or antigens in serum samples, there are the assays of immune-recognition with bound enzyme, more commonly known as ELISA.

In detail, the execution of such tests is performed on 96-well polycarbonate plates (Figure 9) on which are immobilized different molecules, depending on the analyte of interest to bind.

Figure 9: ELISA 96-well polycarbonate microplates

In particular, if the target analyte is an antigen, the wells will be functionalized with the antibody directed towards it, which will be immobilized via the F_c portion in order to expose the F_{Ab} portion, specific for the interaction with the antigen. On the contrary, in case it is necessary to determine an antibody, the wells will be functionalized with the antigen to which it is directed.

In both cases, a specific binding occurs between an antigen and an antibody, followed by the reading step, carried out through a “reading” antibody, labeled with an enzyme, commonly horseradish peroxidase (HRP) or alkaline phosphatase (AP). The latter allows, via an enzymatic detection mechanism based on the processing of a specific substrate, to generate a pectrophotometric signal referable to the concentration of the target antigen or antibody. On the basis of the chemical nature of the antigen to be determined, it is possible to distinguish the ELISA assays in "sandwich" and "competitive", each of which can be applied in direct or indirect mode (Figure 10).

Sandwich ELISA

This test is used for the determination of analytes of protein nature. To this purpose, a primary (capture) antibody, usually monoclonal, it will be immobilized on the wells. During incubation of the sample containing the target antigen, this latter will be immunosorbed on the wells to be

subsequently reacted with a secondary antibody, also specific, but capable of recognizing an antigenic determinant different from that towards which it is directed the capture antibody. In this case, a signal directly proportional to the concentration of the target antigen it will be recorded.

Direct type Sandwich ELISA:

The secondary antibody is directly labeled with enzyme, also acting as a reading antibody.

Indirect type Sandwich ELISA:

The reading antibody is a third antibody, which binds to the sandwich formed by the primary and secondary antibodies. In this case it is not necessary to use a specific antibody, since the third reading antibody (anti-antibody)is able to recognize the F_c of the secondary antibody, referable to species (anti-mouse antibodies, for example).

Competitive ELISA

In this case, the wells are functionalized with the analyte to be searched, which will be immobilized to the substrate. The aim is the establishment of a competition for the interaction with the antibody directed against the analyte, which is established between the latter, possibly present in the sample, and the corresponding bound to the well.

Since all complexes not immobilized are removed in the washing steps, the measured signal is referable to the immobilized immunocomplexes, therefore indirectly ascribable and inversely proportional to the concentration of the target antigen.

The immunosorbed antibodies will be finally detected through a reading anti-antibody, labeled with the proper enzyme.

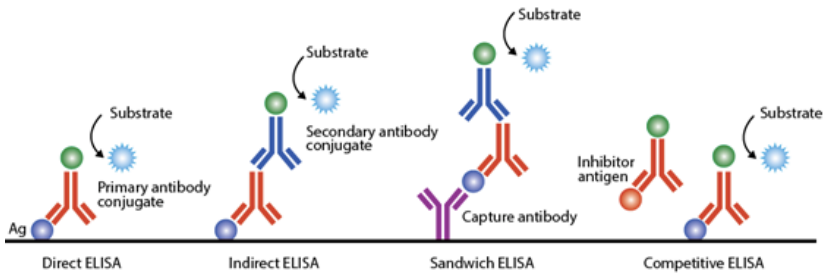

Figure 10: Schematic rappresentation of different ELISA assays, classified as above-discussed.

2.2 From traditional ELISA to the development of immunosensors

In clinical settings, and not only, is progressively increasing the need for rapid, simple, robust and automated analysis methods, used for the continuous monitoring of analytes.

A fundamental need is to to reconcile the suitability with complex biological matrices such as serum, without a pretreatment of the sample, with high levels of accuracy, sensitivity and specificity.

Moreover, frequently clinical analyses are not performed only in highly equipped laboratories, but can also be performed in hospitals, in non-hospital structures by health workers or also at home by themselves patients. It follows, therefore, a particular interest in the design of miniaturized and portable devices, for *in situ* and *real-time* measurements, not only for *routine* investigations in the laboratory, but also for "home made" tests, therefore easy to use and cost- sustainable. Biosensors are sensing devices able to meet these needs, and were object of intensive research and ingegnerization in recent two decades.

In general, a chemical sensor is a device able to transforms chemical informations into analytically useful signals, and is constituted by a chemical or biological receptor for molecular recognition, in association to a certain transduction system. In more details, in the "biosensors", the receptor is a biological element, which can be an enzyme, a peptide, an antibody, etc., able to recognize the analyte of interest. The interaction between the recognition element and the target analyte causes a measurable change in a property of the solution, such as the formation of a product. The transducer converts such change in a quantifiable electrical signal.

When the receptor is an antibody or an antigen and the recognition is based on the specific antigen-antibody interactions biosensors can be defined as immunosensor (Figure 11), which can be considered as the sensoristic transposition of the immunoenzimatic assays, with the same working principles described for the ELISA tests.

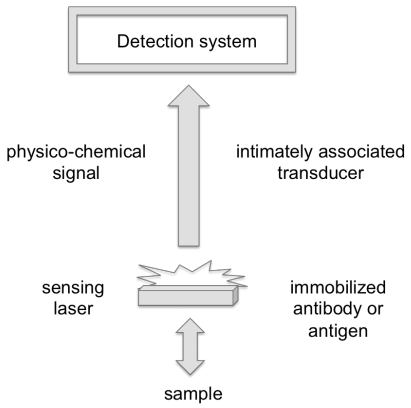

Figure 11: Schematic representation of the operating principle of immunosensors.

3. Biosensors

3.1 Biosenors: state of the art

Biological and biochemical processes have very important roles on medicine, biology and biotechnology. However, it is very difficult to convert directly biological data to electrical signal but, as already mentioned, the biosensors can convert these signals and the biosensors over this difficulty. In recent years, thanks to improved techniques and devices, the diffusion and the application of these products have increased[52].

The first biosensor was described in 1962 by Clark and Lyons who immobilized glucose oxidase (GOD) on an amperometric oxygen electrode surface semipermeable dialysis membrane in order to quantify glucose concentration in a sample directly[53,54]. They described how to make "more intelligent electrochemical sensors" by adding "enzyme transducers as membrane enclosed sandwiches".

According to the IUPAC definition, an electrochemical biosensor is a self-contained integrated device, which is capable of providing specific quantitative or semi-quantitative analytical information using a biological recognition element (biochemical receptor) which is retained in direct spatial contact with an electrochemical transduction element[55].

Considering their structure, biosensors are typically comprised of three components (Figure 12):

1. The bio-recognition element (bioreceptor), that is an immobilized sensitive biological element (e.g. antibody/antigen, enzymes, nucleic acids/DNA probe, cellular structures/cells, or biomimetic materials) recognizing the analyte.
2. The transducer, which converts the variation of the (bio)chemical signal, resulting from the interaction of the analyte with the bioreceptor, into a measurable signal such as an electronic, photonic, thermal or mass signal. The intensity of generated signal is directly or inversely proportional to the analyte concentration. A transducer is used to convert into an electronic one[53].
3. The electronic system, which includes a signal amplifier, processor, and display.

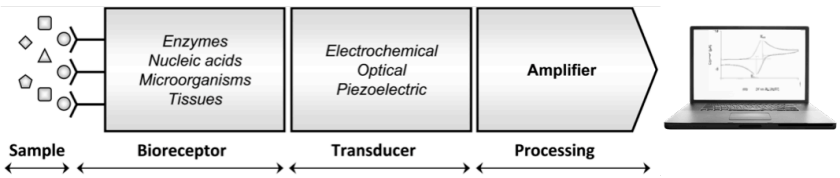

Figure 12: Components of a biosensor

Biosensors are categorized according to the basic principles of signal transduction and biorecognition elements. According to the recognition elements, biosensors can be classified in three classes: molecular biosensors, cellular biosensors, and tissue biosensors. Taking into account the molecular biosensors, they can be further divided in two classes:

. Enzyme biosensors, where the receptor is an enzyme that catalyzes a reaction which involves the targeted analyte.

. Bio-affinity biosensors characterized by either an antibody or an antigen as receptor and are based on antigen-antibody interaction: in this case, they are called immunosensors, as mentioned above.

In addition, depending on the transducing elements, biosensors can be classified as electrochemical, optical, piezoelectric, and thermal sensors[55]. Electrochemical biosensors are also classified as potentiometric, amperometric and conductometric sensors.

3.2 Amperometric electrochemical biosensors

Bioelectroanalysis with electrochemical biosensors is a new area in rapid development within electroanalysis. Usually, electroanalytical techniques have an intrinsic high sensitivity and simplicity that can be combined to miniaturized hardware. The possibility to miniaturize the instrument can pave the way to the engineering and the production of portable, user-friendly and low-cost devices, also applicable to in vivo analysis using some micro-liters of sample. They can be used in clinical analysis, in on-line control processes for the industry or the environment, or even *in vivo* studies.

3.2.1 Amperometric transducers

The amperometric transduction is biologically considered the most consolidated and effective technique. It detects the current that circulates in an electrochemical cell as a result of an applied potential. The required instrument is composed by three electrodes connected to a potentiostat (Figure 13).

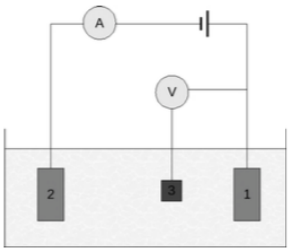

Figure 13: Three electrodes system

Usually, the receptor is immobilized on the working electrode (WE) (commonly gold, carbon or platinum), the potential between the WE and the reference electrode (RE) is fixed at a determined value and then the current, flowing between WE and counter electrode (CE), is measured with respect to time. The applied potential is the driving force for the electron transfer reaction and the current produced is a direct measure of the rate of electron transfer. A lot of analytes are not electrochemically active, thus they can not take part in a redox reaction, not producing an electrical signal. In these cases, a redox mediator is necessary: it is a small molecule capable of accepting and donating electrons generating a product able to give a signal proportional to the concentration of the analyte. As for antibody or antigen determination, an enzymatic label is widely used because it not only produces electroactive species, but also acts as an amplifier; even if only few enzyme-linked antibodies remain bound, the enzyme molecules will produce many signal molecules. Between immunological techniques, these electrochemical devices are really good alternative to the traditional ELISA assays based on optical detection.

In **voltammetry**, a category of electroanalytical method, a constant and/or varying potential is applied and the resulting current is measured. This technique can reveal the reduction potential and the electrochemical reactivity of an analyte and also allows to get analytical (concentration), thermodynamic (redox potential and constants of equilibrium), and kinetic (speed of reaction) informations. One of the most important and widespread applications of voltammetry is the quantitative determination in solution of chemical species that have the ability to be oxidized or reduced, sometimes to levels below the μg/l.

Linear Sweep and Cyclic Voltammetry

Linear-sweep voltammetry (LSV) represents one of the most exploited electrochemical approach, involving a linear scan of potential in either the negative or positive direction. A set of LSV experiments generates a so-called cyclic voltammetry (CV), where anodic and catodic scans are repeated alternately: at the end of the first LSV, the scan is continued in the opposite direction and the cycle can be repeated several times. The resulted faradic current is reported as function of

applied potential generating a cyclic voltammogram. Moreover, an additional nonfaradic current, known as capacitive current (C), is not referable to the active species reacting at the WE, but is directly proportional to the scan rate (ν):

$$i = C \times \nu$$

When applying to the WE a triangular scan a forward process is induced, while under inversion of the sweep direction the backward reaction of the electroactive species occurs (Figure 14).

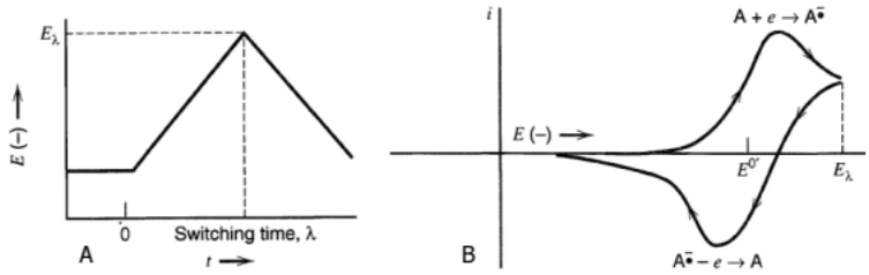

Figure 14: Cyclic potential sweep (A) and resulting cyclic voltammogram (B)

These methods are nondestructive since only a very small amount of the analyte is consumed at the two-dimensional surface of the working and auxiliary electrodes. To perform a cyclic voltammetry experiment a three electrodes cell has to be used since a supporting electrolyte should be present in order to avoid the migration under electric gradient of charged electroactive species. The desired potential must be applied to the WE (which makes contact with the analyte) in a controlled way and to facilitate the transfer of charge to and from the analyte. Since it is extremely difficult for an electrode to maintain a constant potential while passing current to counter the redox events at the WE, a three-electrode configuration allows to apply a potential to the WE respect to the RE and measures the fluxed current between WE and CE. These data are plotted as current (i) versus applied potential (E). As is shown in Figure 15b, during the initial forward scan an increasing overpotential is applied; thus, the faradic current will increase over this time assuming that there are reducible analytes in the system. After the reduction or oxidation potential of the analyte is reached, the forward current will decrease as the concentration of reactive analyte is depleted. The reacted analyte will start to be re-converted to the starting oxidation state during the reverse scan (backward process) depending on the electrochemical reversibility degree of the electrodic process, generating a current of reverse polarity , with respect to the forward process. More reversible is the redox couple, more similar the oxidation peak will be in shape to the reduction peak. Hence, CV data can

provide information about redox potentials and electrochemical reaction rates. All the electrochemical reactions are described, at least in part, from the Nernst equation. This equation correlates the potential of electrode with the concentration of the two species (oxidized, OX and reduced, RED) involved in the electrodic process.

$$E = E^0 + \frac{RT}{nF} \ln \frac{c_{OX}}{c_{RED}}$$

When a potential is applied, the concentration of the OX species decreases at the electrode interface, and will generate a concentration gradient. If the potential becomes more negative, the concentration at the electrode surface of the OX species will decrease and the analyte concentration in the bulk is not equal to that on the electrode surface, generating a driving force for the diffusion of the OX species in a place with less concentration, in order to match the concentrations. This diffusion of the analyte and its oxidation/reduction when reaching the electrode surface, generates a current intensity. If the electron transfer at the WE surface is fast and the current is limited by the diffusion of analyte species to the electrode surface, then the peak current will be proportional to the square root of the scan rate. It follows that, if the OX species moves towards the electrode surface, a reduction current will be generated ($i<0$, catodic current), whereas if the OX species moves far from electrode surface will be produced an oxidation current ($i>0$, anodic current). In nerstian systems, the shape of the cyclic voltammogram depends on the switching potential or how far beyond the cathodic peak the scan is allowed to proceed before reversal. Basically, from a cyclic voltammograms two measured parameters can be obtained: the ratio of peaks currents, i_{pa}/i_{pc}, and the separation of peak potentials, E_{pa}-E_{pc}. If the redox couple is reversible, when the applied potential is reversed, it will reach the potential that will re-oxidize the product formed in the first reduction reaction, producing a current of reverse polarity from the forward scan. If the cathodic sweep is stopped and the current is allowed to decay zero, the resulting anodic i-E curve is identical in shape to the cathodic one, but is plotted in the opposite direction on both the i and the E axis (Figure 15).

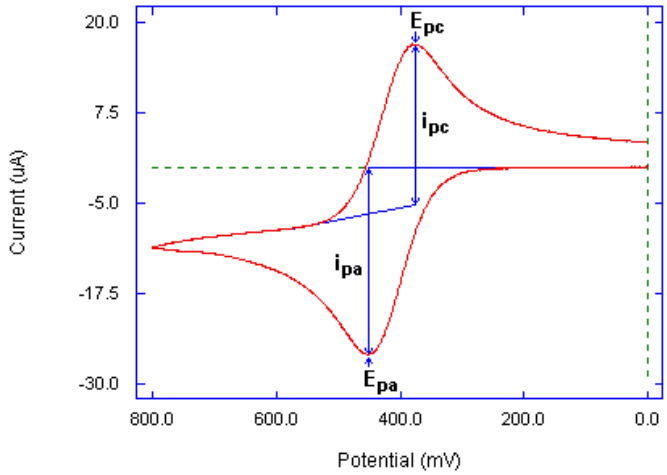

Figure 15: A typical cyclic voltammogram showing the important peak parameters, where ipc and ipa show the peak cathodic and anodic current respectively for a reversible reaction while Epa and Epc are the peak anodic and cathodic potential respectively.

ΔEp is always close to 2.3RT/nF (or 59/n mV at 25°C). For repeated cycling the cathodic peak current decreases and the anodic one increases until a steady-state pattern is attained (ΔEp=58/n mV at 25°C).

Cyclic voltammetry is the most widely used technique for acquiring qualitative information about electrochemical reactions, to study the electrochemical properties of an analyte in solution, and it offers a rapid location of redox potentials of electroactive species.

Differential Pulse Voltammetry

Many forms of potential modulation have been developed in order to increase speed and sensitivity of voltammetric analysis. One of these techniques is the Differential Pulse Voltammetry (DPV) that is often used for ultrasensitive electroanalyses at very low concentration of the target analytes. DPV is a derivative of LSV to which is applied a periodic series of voltage pulses of constant duration and amplitude(stairsteps) obtaining a remarkable improvement of the signal-to-noise ratio. The setup of the system is usually the same as that of standard voltammetry. Basically, the potential between the WE and the RE is changed as a pulse from an initial potential to an inter-level potential and remains at this level for about 5 to 100 milliseconds; then it changes to the final potential, which is different from the initial potential (Figure 16). Measuring the current difference that passes just before and in the last moments of impulse life, a measurement that is much less affected by capacitive current will be obtained. It is thus provided a measure of differential current that generates a voltammogram with a gaussian-shaped peak. The width of the Pulse Amplitude (PA) is important because larger amplitudes will yield a stronger response, but the peak will be broadened and the potential resolution will be inferior. Moreover, larger amplitude can lead to a distortion of

the peaks due to non-linearity effects. The the current flowing between the WE and CE is sampled before and after each pulse and the difference is plotted as a function of potential. Since the capactive current undergoes more rapid decrease over the time, with respect to the faradic (analytically useful) component of the current signal, capacitive current contributions will be expressed as a more or less constant baseline. This method is very sensitive and further improves the detection limit, which are around to 10-100 μg/l.

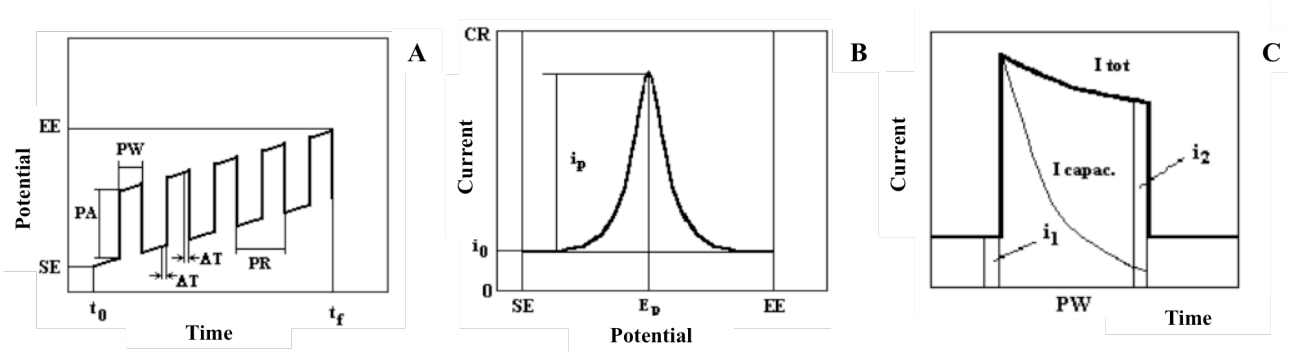

Figure 16: (A) Anodic scanning of potential; (B) Recorded voltammogram; (C) Trend of the current during a pulse.

3.2.2 Amperometry as a bioanalytical platform

Amperometric sensors are useful analytical tools, thanks to their ability to provide important information without damaging the immobilized biological element due to the possibility of performing measurements under physiological conditions comparable to the native environment. Amperometric immunosensors show enormous advantages compared with traditional ELISA assays with spectrophotometric reading. They are indeed characterized by shorter analysis time and by the possibility of implementation on portable, battery-operated devices. Furthermore, immunosensors enable more accurate quantitative or semi-quantitative analysis than those offered by ELISA assays[58].

3.3 Piezoelectric biosensors

3.3.1 Piezoelectric Quartz Crystal (PQC) system

The piezoelectricity was discovered in 1880 by the French physicists Jacques and Pierre Curie. They demonstrated that subjecting a solid crystal surface to mechanical stress by pulling, pressure or torsion, an electric charge is generated and the intensity of potential is proportional to the applied

stress. "*Piezoelectric*" comes from the word *piezen* that means "*press*". The piezoelectric effect is a reversible process and a relationship between mechanical and electrical variables leads to two different types of piezoelectricity: (i) direct piezoelectric effect, which is the internal generation of electrical charge resulting from an applied mechanical force; (ii) reverse piezoelectric effect, that is the internal generation of a mechanical strain resulting from an applied electrical field. In particular, this inverse piezoelectric effect is used in the production of piezoelectric sensors[56,57].

The application of an alternating voltage produces a mechanical vibration of crystal reflecting the variation of the potential during the time. The distortion allows the crystal to vibrate at a particular resonant frequency. In order to produce mechanical vibration an electrode structure is necessary to apply an electric voltage. The crystal has electrodes deposited on both sides. These electrodes are made of a low resistance metal such as silver, gold and aluminium. The electrode also provides a means of attaching the crystal to the mounting structure of the crystal base (Figure 17).

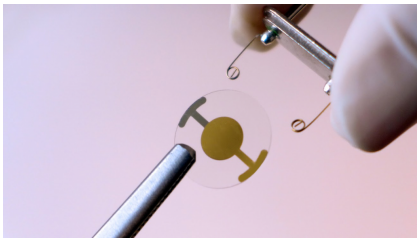

Figure 17: Immagine of a crystal with gold electrodes deposited on both sides and its the mounting structure.

Although a large number of crystals show piezoelectricity, only quartz provides the unique combination of mechanical, electrical, chemical, and thermal properties and is the most common material for oscillator crystals[56]. Each piezoelectric sensor has a particular fundamental frequency that is related to crystal thickness, structure, geometry, cut, dimension and the electrode position. The fundamental frequency ranges from 106 Hz to 109 Hz corresponding to the acoustic wave range, so that they are called also acoustics sensors[57].

3.3.2 "Quartz Crystal Microbalance" as a bioanalytical platform

One of the most used PQC devices, mainly for the sensor application, is the quartz-crystal-microbalance (QCM). In QCM both surfaces are covered by a thin metallic surface, usually gold, deposited under vacuum conditions. Between quartz and gold films there is an intermediate film of either chrome or titanium required for the adhesion of gold to the quartz surface. The fundamental frequency of the crystal can change but usually ranges from 5 to 30 MHz and the resonance frequency of these quartz increases with decreasing thickness.

In order to use a Piezoelectric Quartz Crystal (PQC) system as mass sensor, using its piezoelectric properties, it has to be connected to an oscillator and to a counter (frequency channel). The first one permits the vibration of the crystal applying specific potential, while the latter monitors the frequency and mass variations detected by quartz.

The operating principle of QCM sensors is based on the interaction between the surface of a quartz crystal coated with the sensing layer and the analytes. If a rigid layer behavior is assumed for the crystal, the change in resonant frequency is a function of the mass changes on the surface of the PQC, according with the Sauerbrey equation:

$$\Delta f = -\frac{2f_0^2}{A\sqrt{\rho_q \mu_q}}\Delta m$$

where Δf is the observed frequency change (Hz), f_0 is the fundamental frequency of the PQC, Δm the mass change (g), A is the working surface area of the quartz/electrode (cm^2), ρ_q is the density of quartz and μ_q indicates the shear modulus of quartz for AT-cut crystal.

Concerning the transducers, QCM-based sensors are gaining an increasing interest as competitive tools for biosensing applications and clinical bioassays in liquid phase due to high sensitivity, low cost and real-time output.

3.4 Functionalization of the electrode surface

3.4.1 The recognition element

The real success of affinity biosensors for ultra-sensitive detection depends on the reaction efficiency between the analyte and the recognition element, immobilization of recognition elements on the support surface as well as the choice of transducer and signal probes[59]. Several different recognition elements have been proposed to induce sensitive detection, such as antibodies, antibody fragments, or aptamer that should possess both a high binding affinity for the target and good interfacial stability. Concerning the antibodies, both polyclonal and monoclonal immunoglobulins can be used. Polyclonal antibodies are generated from a range of immune cells and may bind to the target at different location and/or with different binding affinities. On the other hand, monoclonal antibodies are made by identical immune cells that are all clones of a unique parent cell and they bind the same epitope with equivalent affinity, providing higher selectivity or more consistent assaying than polyclonal antibodies. Other recognition elements are nucleic acid (DNA or RNA), chemically more stable than antibodies, antibody mimic proteins (AMPs), non-antibody recognition

proteins (peptide aptameters), or synthetic receptors such as molecularly imprinted polymers (MIPs).

3.4.2 Recognition element immobilization

The design and construction of a sensing interface depend critically on how the recognition elements are integrated onto the transducer. The immobilization methodologies are dependent on the physical and chemical characteristics of the transducer element and the environment of the operation. Current devices are made by noble metals (Au, Ag, Pt), carbon materials (glassy carbon, carbon paste, nanotubes) or semiconductors (Si, nanotube, nanowires) and a lot of methods can be used for immobilize the receptor on the electrode surface. This is the most critical point in the realization of a biosensor. In the case of protein molecules such as enzymes and antibodies, in particular, it is necessary that the quaternary structure remains unchanged, with the preservation of a certain conformational freedom, and the prevention of denaturing processes, in such a way that it is kept unchanged their function. Moreover, it is very important that the immobilization is highly efficient and reproducible, so allow the effectiveness and standardization of the assay. The commonly used method for the immobilization of biological elements are described as follows[60,61]:

• Chemosorption
• Covalent immobilization
• Cross-linking
• Bio-specific interaction

The easiest and low-cost method with good performances is the chemosorption that is characterized by the intercation of atoms, ions or functional groups of the receptor from the solution to the surface, on the basis of weak non-covalent interactions such as Van der Waals forces, dipolar interactions or hydrogen bonding. Conversely, a covalent immobilization is often necessary and may result in better biomolecule activity, reducing non-specific adsorption, and inducing higher stability. The immobilization reaction should occur quickly, the reagents for immobilization should be used at low concentration and the ligands must be immobilized in an oriented and homogeneous way, using, for example, functional groups including amines, thiols, carboxylic acids and alcohols. Furthermore, high surface density may generate steric interference between the covalently immobilized ligand molecules, preventing access to target molecules. Therefore, correct orientation of ligand molecules on the surface and the use of spacer arms are other critical parameters.

For this purpose there are some approaches as the cross-linking technique, involving the use of bifunctional or multifunctional reagents (such as glutaraldehyde or carbodiimide[62]) which are

capable to bind the electrode substrate with a functional group and the recpetorial biomolecule with the other one. Another possibility is the use of native or engineered protein cysteine residues that allows the covalent binding to noble metal surfaces, such as gold.

3.4.3 Nanostructured materials

Nanotechnology ("nanotech") is the engineering of functional systems at the molecular scale, able to create many new materials and tools with a wide range of applications, such as in medicine, electronics, biomaterials energy production, and consumer products. Nanotechnology is defined by The National Nanotechnology Initiative as the manipulation of matter with at least one dimension sized from 1 to 100 nanometers that is comparable to many biological macromolecules such as antibodies, enzymes, viruses and DNA plasmids.

On the other hand, despite their great potential, as for many new technologies also for the nanotech are raised concerns about the toxicity and environmental impact of nanomaterials[63].

Nanostructured materials are endowed with particular physico-chemical properties that distinguish them from traditional bulk materials, in particular, the increase in the surface / volume ratio, with consequent exponential increased in the surface area available at the interphase. They have also particular optical, magnetic and electrical properties. There are several examples of nanostructures, which differ in type and size, for example the carbon nanotubes, characterized by nanoscale diameters, or the nanotissue, which have nanometric thickness. There are, furthermore, materials that exhibit all three dimensions of the nanometer order, such as the nanoparticles.

In detail, metal nanoparticles from noble elements such as Au, Ag, Pt, Pd, Ru have further advantages compared to other nanomaterials, in terms of high surface area, high mechanical strength, lightness, chemical and thermal stability, conductivity, biocompatibility, electric properties, magnetic and optical properties due to their size. They may have different functions including the immobilization of biomolecules, the catalysis of electrochemical reactions, the enhancement of the electronic transfer, the labeling of biomolecules and direct participation in chemical reactions as reagents.

Nanomaterials are therefore, extremely versatile when used in electrochemical devices, in particular for sensors and biosensors, with the possibility to significantly improve the sensitivity, due to an effect of amplification of the electron transfer phenomena[64-66].

3.4.4 Carbon nanotubes

The discovery of carbon nanotubes (CNTs) in 1991 opened up a new era in materials science. These are high performing structures that have more fascinating electronic, magnetic and mechanical properties. CNT are at least 100 times stronger than steel, but only one-sixth as heavy, so nanotube fibers could strengthen almost any material. Nanotubes can conduct heat and electricity far better than copper.

A carbon nanotube is made by one or more of graphite superimposed sheets folded to form hollow cylindrical structures, having a diameter measuring on the nanometer scale (about 10,000 times smaller than a human hair), and with properties that depend on the atomic arrangement, on the diameter and on the length of the tubes.

CNTs present unique properties because the bonding between the atoms is very strong and the tubes can have extreme aspect ratios. The characteristics of nanotubes can be different depending on how the graphene sheet has rolled up to form the tube causing it to act either metallic or as a semiconductor. The graphite layer that makes up the nanotube looks like a continuous unbroken hexagonal mesh and carbon molecules at the apexes of the hexagons (Figure 18). A carbon nanotube can be as thin as a few nanometers yet be as long as hundreds of microns. Carbon nanotubes have many structures, differing in length, thickness, and number of layers.

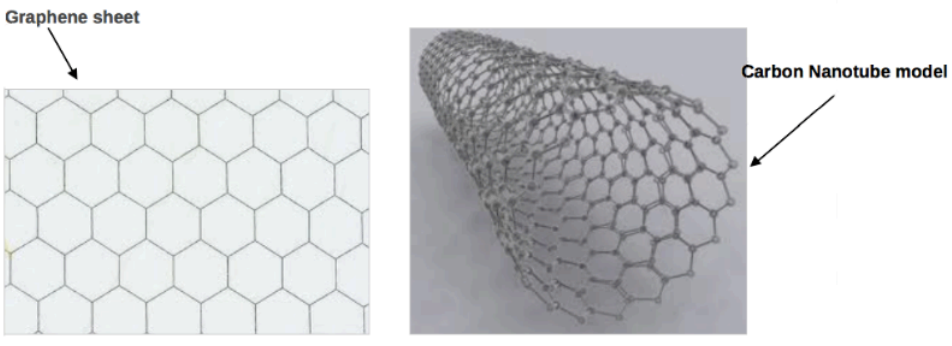

Figure 18: Schematic rappresentation of carbon nanotube made from rolled graphene sheet

There are many different types of carbon nanotubes, but they are normally categorized as either single-walled (SWNT) or multi-walled nanotubes (MWNT) (Figure 19)[52]. A single-walled carbon nanotube has only one layer, or wall. Multi-walled carbon nanotubes are instead a collection of nested tubes of continuously increasing diameters, that can range from one outer and one inner tube (a double-walled nanotube) to as many as 100 tubes (walls) or more. Each tube is held at a certain distance from either of its neighboring tubes by interatomic forces. As in the fullerenes, the circular curvature causes rehybridization of σ and π bonds so the π bond is more localized with respect to

graphite. This gives greater mechanical strength nanotubes, thermal and electrical conductivity, along with the ability to be more biologically and chemically active.

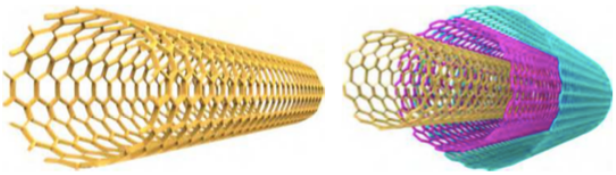

Figure 19: Single- and Multi-walled Carbon Nanotubes

3.4.5 Gold nanoparticles

Regarding the development of biosensors, among the nanoparticles of noble metals, the most frequently studied are undoubtedly the gold nanoparticles, due to their stability and high reachable performance. In general, the nanoparticles represent an ideal substrate for the immobilization of biomolecules and have been widely investigated for their potential application in the development of biosensors, especially for biomarkers detection because of their large surface to volume ratio, chemical stability and high biocompatibility. In particular, the immobilization of protein molecules, such as antibodies or enzymes on gold nanoparticles, by is highly efficient , since it is based on a very stable bond, with the maintenance, at the same time, of biological activity of the bioreceptor and of a good conformational freedom. The immobilization takes place by chemisorption, occuring through interactions between gold substrate and sulphur from the cysteine residues present on the protein molecules, thanks to high Au-S affinity, energetically comparable to a covalent interaction[64,67,68].

Preparation of nanogold is usually performed in solution from tetrachloroauric acid ($HAuCl_4$), in the presence of a reducing agent, also acting as encapsulating reagent for the colloidal suspension of nanoparticles. Another approach to obtain gold nanoparticles directly immobilized on glassy carbon electrodic substrates is the electrochemical reduction, where the application of a negative potential, under potentiostatic, potentiodynamic or galvanostatic conditions, allows the electrodeposition of gold nanoparticles owing to the reduction from Au^{3+} to Au metallic state.

The optical properties, the excellent biocompatibility, conductivity, catalytic properties, high surface-to-volume ratio and high density of AuNPs lead to a wide application of these particles in the development of optical, electrochemical and piezoelectrical biosensors[69].

Focusing on electrochemical and piezoelectrical biosensors, the roles of the gold nanoparticles are

different.

Concerning electrochemical biosensors, the AuNPs can act as:

1. Electron transfer "electron wires". The conductivity properties of AuNPs enhance the electron transfer between the active center of most reductases and the electrodes, acting as "electron wires". Often, indeed, the active center of most reductases is surrounded by protein shells and the electron transfer is blocked causing poor analytical performances.
2. Immobilization platform. As already mentioned, AuNPs thanks to their high surface free energy allow the adsorption of biomolecules retaining their bioactivity and stability and, sometimes the recognition elements are linked to the nanoparticles by the use of sulfur atoms or via thiol linkers. In addition, AuNPs are often conjugated with other nanomaterials such as carbon nanotubes to improve their binding capacity.
3. Electrocatalysts. It has been recently demonstrated that quantum scale dimension and the large surface-to-volume ratio can decrease overpotentials of many analytically electrochemical reactions allow reversibility of some redox reactions allowing the development of enzyme-free biosensors.

As for piezoelectric biosensors, the high density of AuNPs can amplify the mass change on the crystals surface, thus improving significantly analytical sensitivity. Unlike to what happens using bulk materials, the adsorption of biomolecules on nanostructured surfaces does not causes their denaturation, thanks to the high biocompatibility of the nanoparticles.

3.4.6 Screen-printed electrodes

To promote the portability of biosensors, in recent years were developed the Screen-Printed Electrodes (SPEs), characterized by a low manufacturing cost and the possibility of a massive production (Figure 20). These electrodes are characterized by a ceramic or plastic support on which the three electrodes of the amperometric sensor are printed with different inks, according to the use. The big advantage, in addition to miniaturization, is the ability to functionalize the chips differently, for example with gold or gold nanoparticles in serial production, thanks to the planarity of the support. The combination of all three electrodes needed for the amperometric measurement allows to recreate the entire electrochemical cell on the electrode, requiring very small volumes (10-50µl) of sample for the execution of the analysis. Furthermore, SPEs are disposable, thanks to their low cost (≈ 2€ for piece). In the field of research devices, the SPEs are usually purchased with the proper electrode substrate, and the sensing molecule as well as other enhancing nanomaterials are

fixed/deposited during the development stage of the study. Conversely, the ready-to-use SPEs commercially available are previously functionalized with the chemical or biological receptor, properly protected by blocking protein films.

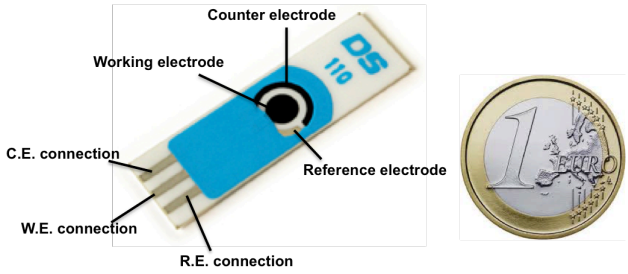

Figure 20: Screen-Printed Electrodes

3.4.7 Linker for covalent immobilization

In order to improve the stability and control of the distribution and orientation of the species on the electrode surface, an alternative at the direct immobilization of biomolecules on gold it is represented by the use of heterofunctional linkers, presenting one extremity capable of interact with the substrate and the other one capable of covalently bind the recognition element of interest, with the possibility to reach an efficient and reproducible functionalization, in addition to an higher conformational control, in terms of proper orientation of the bioreceptor.

For the immobilization of protein molecules such as antibodies and enzymes functional groups able to genarate amide bonds, such as the carboxyl groups, are needed on the sensing surface.

For this purpose, it is possible to use different types of linkers.

One of the more common approach is the use of Self-Assembled Monolayer (SAM), obtained from alkylthiols. Such molecules must be functionalized with carboxyl groups at the opposite extremity with respect to the thiol group.

Another approach is caracterized by the use of some biologically active proteins, such as Protein A or G, commonly used as a binding material to orientedly immobilize antibodies due to their ability to specificaally bind the Fc fragment of the antibodies, in order to leave the FAb moieties available for the immunorecognition of the target antigen[70-72]. As protein A can be firmly chemosorbed onto gold surface, through its cysteine residues[73].

3.5 Biosensors as diagnostic devices for p53 detection: state of the art

One of the most common analytical approaches for the determination of p53 is represented by immunological tests, principally ELISA assays.

On the basis of the increasing clinical interest for the determination of this protein in cell lysates and biological fluids, a variety of analytical approaches have been developed and proposed. They comprise matrix-assisted laser desorption/ionization time-of-flight mass spectrometry combined to high-performance liquid chromatography pre-fractioning[47], immunochemical methods[48,49] and surface-enhanced Raman spectroscopy[50]. Concerning sensing devices, field effect transistors[74] as well as surface plasmon resonators[51] have been investigated as biologically addressable substrates for the selective determination of p53.

In recent years, biosensors have been explored for their application in biological field because match the fundamental needs required for the screening analysis of biological samples, in terms of reliability, simplicity of operation and instrumentation, time and cost sustainability, associated to good sensitivity and high specificity assured by targeted antibodies.

Amperometric immunosensors are furthermore very versatile tools for rapid and user-friendly screening analysis[75] of biomarkers of clinical concern, thanks to their compatibility with portable and compact instrumentation, exploiting disposable screen printed electrodes as sensing substrates[76,77].

Despite the strong interest, to date, a limited number of publications reported about amperometric immunosensors aimed to the determination of p53 in samples of clinical concern. All these immunodevices are based on the working principle of the sandwich Enzime Linked ImmunoSorbent Assay (ELISA), involving the use of a capture antibody, properly immobilized as bioreceptor on the electrodic surface, paired with a secondary antibody able to recognize a different epitope of the target antigen. In most cases the secondary antibody is not available as conjugated with the labeling enzyme, requiring the use of a third enzyme-labeled reading anti-antibody. A graphene-based immunosensor, was developed by Xie et al in 2011[78], for electrochemical quantification of p53 phosphorylated on serine 15 (phospho-p53^{15}), based on sandwich immunoassay involving a phospho-p53 capture antibody, a biotinylated phospho-p53^{15} detection antibody and horseradish peroxidase (HRP)-labeled streptavidin. In the same year, Du et al. reported about a new electrochemical immunosensor also aimed to ultrasensitive detection of phosphorylated p53 at serine 392 (phospho-p53^{392}) based on graphene oxide (GO) as nanocarrier in a multienzyme amplification strategy[79]. Again, phospho-p53^{392} was the target of a nanomaterial enhanced disposable immunosensor using enzyme functionalization of carbon nanospheres as a

signal amplification label and magnetic beads coupled with screen printed carbon electrodes as electrochemical transducers[80]. More recently, concerning immunosensors of unphosphorylated p53, the target protein was sandwiched between biotinylated capture anti-p53 immobilized on gold nanoparticles/graphene oxide electrodic surface via thiolated GO/streptavidin-Au NPs and secondary anti-p53 labeled with horseradish peroxidase (HRP), realizing a complex but ultrasensitive electrochemical immunosensor[81].

Purpose of the work

The purpose of the present study is the development of a diagnostic device, based on disposable nanostructured substrates, for the determination of the p53 protein, as clinical evidence of bladder cancer.

Detection of p53 tumor suppressor gene is important in early cancer diagnostics because alterations in the gene have been associated with carcinogenic manifestations in several tissue types in humans. In particular, clinical studies have shown that the development of a kind of bladder cancer, the Bladder Transitional Cell Carcinoma (BTCC), can lead to a significant overexpression of p53 in urine due to the high contact surface between the epithelial cancerous tissues and this biological fluid. Therefore, p53 can be considered as a biomarker of crucial importance, to determine the presence of the disease and its stage of development, as well as for the optimization of therapeutic strategies.

To date, diagnostic techniques used for its determination require long run times and high costs. Among these, ELISA tests represent screening methods of simple, sensitive and specific, applicable to simultaneous analysis of a high number of samples. However, they require dedicated instrumentation and allow mainly a qualitative and semi-quantitative evaluation. A valid alternative approach is represented by the immunosensors, an instrumental transposition of ELISA assays, which in recent years are in wide development since they offer the advantage of combine the high specificity ensured by the antigen-antibody interaction, with the sensitivity of sensing devices used as detection systems. Compared to classical methods, they allow to perform analysis in a lower time and, thanks to the use of small instrumentation, are suitable for large scale production of low-cost portable devices, also for a out-of-hosital use (including self-diagnosis).

Concerning p53, a limited number of studies dealing with amperometric immunosensors were published and are mainly based on the working principle of the "sandwich" type of ELISA assay.

Within this context, the immunosensor developed in this project represent an innovative approach for the determination of p53 in urine, in terms of both methodological and applicative aspects .

The development of the immuno-device has involved the following objectives:

1. Choice of the more appropriate sensing substrate, focused on disposable Screen-Printed Electrodes (SPEs)
2. Identification of the more suitable strategies for the immobilization of the biological sensing element on the surface of the biosensor, in order to keep its functionality and biological activity. This is one of the most critical points in the realization of a biosensor and

we have exploited, for this purpose, the intrinsic characteristics of nanostructured materials.

3. Identification of the best method of detection and quantification of the target protein. An immunosensor, just like immunoassays, can be based on both competitive or sandwich approach.
4. Optimization of the conditions used for the fabrication of the device and for the execution of the electrochemical immunoassay. For this purpose we applied a multivariate approach, by a set up of a two-factor three-level experimental design.
5. Validation of the device on real samples of clinical concern, such as urine, in order to evaluate the suitability of the immunosensor as rapid and non-invasive screening tool for early diagnosis of bladder carcinoma. In the absence of real clinical samples for paients, we used Synthetic Urine spiked with p53 in order to assess the response in biological matrix.

Again, for validation purpose a home-made spectrophotometric competitive ELISA assay has been developed and tested on 96-wells polycarbonate plates, in order to highlight the improvement of the performance allowed by the use of nanostructured sensing devices.

The sensoristic transposition has confirmed the potential of these devices that, if compared with conventional ELISA, showed undoubted advantages in terms of versatility, portability of the instrumentation, and analytical sensitivity.

The experiments carried out have shown very promising results, foreshadowing the competitive immunosensor as an analytically robust diagnostic tool, valuable for implementation of screening and follow-up programs in patients with urologic malignancies.

Experimental

1. Instrumentation

- Potentiostat *Eco chemie electrochemical workstation µAutolab type III* (Figure 1), managed by *GPES 4.9 software*: used for the reading of the assays.

Figure 1: Potentiostat µAutolab type III (Metrohm)

- *Dropsens* Screen-Printed Carbon Electrodes (SPCEs), modified combining Carbon Nanotubes with Gold Nanoparticles (CNT-GNP) (Figure 2).

  Ceramic substrate: L33 x W10 x H0.5 mm

  Electric contacts: Silver

  The electrochemical cell consists on:

  Working electrode: CNT-GNP/Carbon

  Auxiliary electrode: Carbon

  Reference electrode: Silver

Figure 2: SPCE CNT-GNP 110D (Dropsens)

- *Dropsens* Interface SPEs – potentiostat (Figure 3).

Figure 3: Boxed Connector for Screen-Printed Electrodes

- Microplate Reader: *EZ Read 400* (Figure 4), used to read 96-well microplates for ELISA assays.

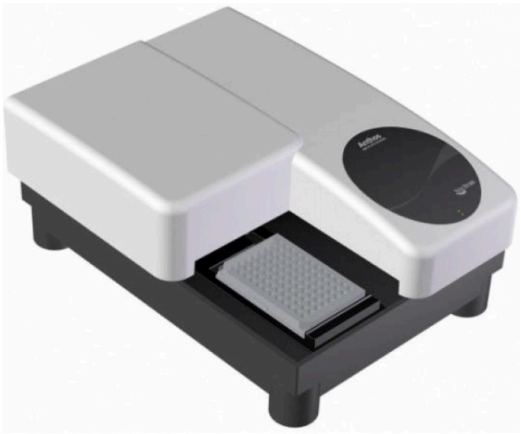

Figure 4: Microplate reader EZ Read 400 (Biochrom) and inserted a 96-well microplate (Abcam)

- Eppendorf micropipettes: used to withdraw the necessary reagent volumes
- pH meter: *pH 1000 L, pHenomenal®*
- Centrifuge *MPW-260R*: for centrifugation Eppendorf tubes
- Precision balance: *Sartorius*
- Vortex Continental Equipment
- Ultrasonic cleaner VWR
- QCM system: piezoelectric Quartz (Institute for Microelectronics and Microsystems, CNR, Rome), modular microbalance with dedicated flow cell for on-line measurements (*Bioage*), *EUREKA support* (*Bioage*), *Software EUREKA* (*Bioage*), peristaltic pump *323-Du* (*Watson e Marlow*)

2. Reagents and standards

- **Reagents for the Immunosensor development**

Reagent	**Source**
Recombinant human p53 full-length protein (200 μg/mL)	Abcam
Mouse monoclonal Anti-p53 Antibody (DO-1) raised against aa 11-25 of p53 of human origin. Isotype IgG2a	Santa Cruz Biotechnology
Mouse monoclonal Anti-p53 Antibody (DO-7) raised against aa 37-45 of p53 of human origin. Isotype IgG2b (1mg/mL)	Abcam
Horseradish peroxidase (HRP) conjugation kit	Abcam
Alkaline Phosphatase-conjugated secondary Rabbit Anti-Mouse IgG (RAM-AP) (1mg/mL)	Abcam
Albumin from bovine serum (BSA)	Sigma-Aldrich
Natural Full length Protein A (200 μg/mL)	Abcam
Surine™ Negative Urine Control, analytical standard	Sigma-Aldrich
Dimethyl pimelimidate (DMP)	Sigma-Aldrich
Trizma ® (HCl)	Sigma-Aldrich

- **Reagents for the preparation of incubation and washing solutions**

Reagent	**Source**
Trizma ® base	Sigma-Aldrich
Tween-20	Sigma-Aldrich
NaCl	Sigma-Aldrich
KCl	Sigma-Aldrich
KH_2PO_4	Carlo Erba
$Na_2HPO_4 \cdot 12H_2O$	Carlo Erba
$MgCl_2$	Carlo Erba
Triethanolamine (THEA)	Sigma-Aldrich

- **Reagents for the preparation of immunosensor reading buffer**

Reagent	**Source**
$Na_2HPO_4 \cdot 12H_2O$	Sigma-Aldrich

NaOH	Sigma-Aldrich
Acetic acid glacial	Sigma-Aldrich
Thionin acetate salt	Sigma-Aldrich
H_2O_2, 30%	Sigma-Aldrich
DropSens® Hydroquinone Diphosphate (HQDP)	Metrohm Italiana
Trizma® base	Sigma-Aldrich
$MgCl_2$	Carlo Erba

- **Reagents for ELISA assay**

Reagent	**Source**
Na_2CO_3	Carlo Erba
$NaHCO_3$	Carlo Erba
NaOH	Sigma-Aldrich
Alkaline phosphatase yellow, *p*-nitrophenyl phosphate disodium salt (PNPP), ready to use liquid substrate for ELISA	Sigma-Aldrich

3 Incubation and washing solutions/buffers

- **PBS 10x (phosphate buffered saline) pH=7.4**
  - NaCl (1.37 M)
  - KCl (0.027 M)
  - KH_2PO_4 (0.015 M)
  - $Na_2HPO_4 \cdot 12H_2O$ (0.08 M)

  The solution is diluted before use to 1x

- **Tween-20 1%**
  - Tween-20, bring to final volume with distilled water

- **PBS-T**
  - PBS 1x (prepared by dilution of PBS 10x in distilled water)
  - Tween-20 1% to a final concentration of 0.05% (*v/v*)

- **TRIS buffer pH=7.4**
  - Trizma® base (0.1 M)
  - $MgCl_2$ (0.02 M)

- **TRIS-T**
  - TRIS 1x (prepared by dilution of PBS 10x in distilled water)
  - Tween-20 1% to a final concentration of 0.05% (*v/v*)

- **Solutions for the funzionalization of the electrode (for sandwich and/or competitive assays)**

  - Protein A solution
    - Protein A solution is prepared by diluting the stock solution in PBS 1x at the optimal concentration (as discussed in chapter ***Results and Discussion***)

  - Triethanolamine (THEA) solution pH=8.2
    - THEA 0.2 M

    Fill to final volume with distilled water

  - Dimethyl pimelimidate (DMP) solution in THEA
    - DMP 20 mM

    Fill to final volume with THEA solution

  - Quenching solution pH=7.5
    - TRIS-HCl 50 mM in distilled water

  - Blocking solution
    - BSA 20 mg/mL in PBS 1x

  - p53 solution

    p53 solutions are prepared by dilution of the stock solution in PBS 1x at the concentration of interest (as discussed in chapter ***Results and Discussion***).

- Anti p53 (DO-7) antibody solution

  DO-7 solutions are prepared by dilution of the stock solution in PBS 1x at the concentration of interest (as discussed in chapter ***Results and Discussion***).

- Anti p53 (DO-7)-HRP antibody solution

  DO-7-HRP solutions are prepared by dilution of the stock solution in PBS 1x at the concentration of interest (as discussed in chapter ***Results and Discussion***).

  Anti p53 DO-7 antibody was previously conjugated with the Horseradish peroxidase enzyme following the protocol provided by the specific commercial HRP conjugation kit.

- Anti p53 (DO-7)-ALP antibody solution

  DO-7-ALP solutions are prepared by dilution the stock solution in PBS 1x at the concentration of interest (as discussed in chapter ***Results and Discussion***).

- Rabbit Anti-Mouse IgG (RAM-ALP) solution

  RAM-ALP solutions are prepared by dilution of the stock solution in PBS 1x at the concentration of interest (as discussed in chapter ***Results and Discussion***).

- **Solutions for the electriochemical immunoassay reading**

  - **"Reading buffer" for thionin acetate pH=6.8 (when using HRP-labeled Ab)**
    - $Na_2HPO_4 \cdot 12H_2O$ (0.05 M)
    - NaOH (0.065 M)
    - Glacial acetic acid (0.0965 M)
    - Add NaOH 2.5 M to raech a pH=6.8 and fill to final volume with distilled water.
    - Shortly before use, add 70 mg of thionin acetate (0.5 mM) and subject the solution to magnetic stirring and sonication to facilitate the solubilization.

  - H_2O_2 solution (0.5 M)
    - H_2O_2 30 %
    - Fill to final volume with distilled water

- **<u>"Reading buffer (RB)" for HQDP pH=9.8 (when using AP-labeled Ab)</u>**
  - Trizma® base (0.1M)
  - $MgCl_2$ (0.02 M)
  - Shortly before use, add 1mg/mL of HQDP to obtain the reading solution and subject the solution to vortex and sonication to facilitate the solubilization.

- **Solutions for the ELISA plate functionalization**

  - <u>Bicarbonate coating buffer for the p53 immobilization on 96-well microplate pH=9.6</u>
    - Na_2CO_3 (0.028 M)
    - $NaHCO_3$ (0.071 M)

  - <u>p53 solution</u>

    p53 solutions are prepared by dilution the stock solution in PBS 1x at the concentration of interest (as discussed in chapter ***Results and Discussion***)

  - <u>Anti p53 (DO-7) antibody solution</u>

    DO-7 solutions are prepared by dilution the stock solution in PBS 1x at the concentration of interest (as discussed in chapter ***Results and Discussion***)

  - <u>Rabbit Anti-Mouse IgG (RAM-ALP) solution</u>

    RAM-ALP solutions are prepared by dilution the stock solution in PBS 1x at the concentration of interest (as discussed in chapter ***Results and Discussion***)

- **Solutions for the ELISA reading**

  - **<u>Reaction substrate for ALP enzime</u>**
    - "Alkaline phosphatase yellow liquid substrate", ready to use

  - <u>Stop reaction solution</u>
    - NaOH (2.5 M)

4 Protocols

Immunosensors were assembled on DropSens disposable Carbon Nanotubes/Gold Nanoparticles-modified Screen-Printed Electrodes (CNT/GNP-SPCEs).

4.1 Sandwich immunosensor set up

1. **Immobilization of Protein A**

   To assure the proper orientation of the catching antibody, working electrodes of CNT/GNP-SPCEs were incubated with Protein A solution by drop-casting of 30 μl of its prepared solution, at a concentration of 200 μg/mL. Incubation is carried out for 6 hours at room temperature (RT), followed by washing with PBS 1x buffer (x3) and careful drying of the electrodes using a nitrogen flow.

2. **Anti p53 (DO-1 clone) capture antibody incubation**

   For this purpose, working electrodes were drop-casted with 30 μl of the antibody solution to the concentration of 20 μg/mL (as discussed in chapter ***Results and Discussion***) at +4°C overnight.

3. **Crosslinking**

   The antibody-functionalized electrodes were subjected to a cross-linking procedure using dimethyl pimelimidate (DMP) as homobifunctional crosslinker. The cross-linking was carried out by casting 30 μl of solution of DMP dissolved in aqueous triethanolamine on each electrode for an incubation time of 30 min at RT.

4. **Quenching**

   The reaction was quenched by drop-casting of 30 μl of TRIS-HCl solution, for 15 minutes at RT.

5. **Blocking**

   A blocking treatment aimed at preventing unspecific responses during the sample incubation was carried out by casting 30 μl of a 20 mg/mL solution of bovine serum albumin (BSA) dissolved in PBS on each electrodes for an incubation time of 60 minutes at RT.

6. p53 protein incubation

Immunoassay were carried out by properly diluting p53 stock solution in PBS 1x at different wanted concentrations (see chapter ***Results and Discussion***) and incubating electrodes with 30 μl of the sample for 1 hour at RT.

The electrodes were then carefully washed to remove unspecifically bound antigen by washing with PBS-T buffer (x3) followed by PBS 1x (x2).

The addition of the anionic surfactant Tween-20 to the first washing solution proves to be highly effective to eliminate the aspecific response in this type of applications. In detail, it is necessary to avoid contamination between the electrodes.

The last wash in PBS 1x allows to eliminate any residues of surfactant present on the immobilized biological molecules on the electrode surface.

7. HRP-conjugated anti-p53 (DO-7-HRP) incubation

In order to detect the antigen (p53) immobilized on the electrodic surface, the immunosensor was incubated for 1 hour at room temperature with 30 μl of a solution of the HRP-conjugated reading antibody, to the concentration of 20 μg/mL in PBS 1x.

8. Reading of the immunoassay

The reading of the assay was performed by cyclic voltammetry (CV) measurement carried out with the sandwich functionalized electrodes in the solution of thionin acetate, under the following operating conditions:

CV reading was performed by scanning the potential between -0.2 and +0.6 V at a scan rate of 50 mV/s. After recording a first measurement in the presence of the only thionine in solution, a stoichiometric amount of H_2O_2 0.5 M was added to the solution and the cyclic voltammograms were acquired again. This allow to record the cathodic *shift* due to the activity of the HRP enzime conjugated to the reading antibody, related to the concentration of the antigen in the sample used for the incubation.

All electrochemical measurements were performed with mAutolab III electrochemical workstation (EcoChemie, Utrecht, NL) equipped with GPES 4.0 version customized software.

4.2 QCM system

Measurements were performed using an Eureka instrument (BioAge s.r.l., Lamezia Terme, CZ, Italy), consisting of a base containing the measurement electronics and a standard measure chamber which contains the quartz crystal. As for the crystal, a 10 MHz AT-cut piezoelectric quartz crystal chips with gold electrodes on both sides (crystal diameter, 13.9 mm; crystal thickness, 160 μm; gold electrodes diameter, 6.0 mm) was exploited. Eureka is self-powered only by the PC USB port and all measurements were performed at 25°C in a flow-through mode under flow laminar conditions using a peristaltic pump (3 rpm). The acquisition speed was set to 2 frequency samplings for second.

4.3 Competitive immunosensor setup

1. **Electrodes funtionalization with p53**

   CNT/GNP-SPCEs were drop-casted with 10 μl of the recombinant human p53 protein solution properly diluted in PBS 1x to a final concentration of 5 μg/mL, allowing to immobilize the protein on nanoparticles, at +4°C overnight.

2. **Blocking**

   After removal of unreacted p53 by careful washing with PBS-T (x3) and PBS (x2), a blocking treatment, aimed at preventing nonspecific responses during sample incubation, was carried out by casting 30 μl of 20mg/mL solution of BSA dissolved in PBS on each electrode at room temperature for 1h, followed by washing with PBS buffer (x3).

3. **Competitive immunoassay**

   Thereafter, the p53-modified CNT/GNP-SPCEs were used to carry out the competitive electrochemical immunoassay. Standard solutions (30 μL) were mixed with 3 μL of ten-fold concentrated anti-p53 solution in PBS in order to reach the proper optimized value (2.5 μg mL-1) in the solution to be used for immunocompetition experiments. The mixture was transferred to the working electrode of the immunosensor and the competition reaction was allowed to take place for 1h at room temperature. Because of the ability of p53 to inhibit antibody binding to the immobilized protein, increasing analyte concentration will reduce the amount of anti-p53 bound to the modified immunosensor surface.

4. AP-conjugated Rabbit Anti-Mouse IgG (RAM-AP) incubation

After the immunocompetition, the sensors were carefully washed with TRIS-T (x3) and TRIS (x2) to remove nonspecifically bound molecules and next the anti-p53 immobilized on the electrodic surface was detected using Alkaline Phosphatase-conjugated Rabbit Anti-Mouse IgG (RAM-AP) as secondary antibody; for this purpose each immunosensor was incubated at room temperature for 1 h with 30 μl of a RAM-AP solution, diluted 1:1000 in TRIS buffer from the original stock solution (1mg/mL).

Finally, carefully washings with TRIS-T (x3) and TRIS (x2) were performed in order to remove unreacted RAM-AP.

5. Reading of the immunoassay

Competitive immunoassays were performed using differential pulse voltammetry (DPV) as a method of electrochemical detection, scanning the potential between -0.5 and +0.3 V, with a pulse amplitude of 0.05 V, a step potential of 0.005 V and a pilse time of 100 ms. Non-electroactive hydroquinone diphosphate (HQDP) was used as enzyme substrate, since alkaline phosphatase (AP)-promoted dephosphorylation yields electroactive hydroquinone (HQ) that is in turn oxidized to quinone (Q) during the DPV scan, giving the p53-related analytical signal. A 1 mg/ml solution of HQDP dissolved in RB was used as reading solution. After drop-casting of the reading solution on the sensor, an equilibration time of 150 s and a preconditioning stage of 30s at -0.5 V were applied prior to run DPV in order to reach an exhaustive enzymatic dephosphorylation and to preconcentrate HQ in its reduced form.

The linearity of the response was explored performing three replicated indipendent measumerements (from different electrodes) for each p53 concentration investigated.

All electrochemical measurements were performed with mAutolab III electrochemical workstation (EcoChemie, Utrecht, NL) equipped with GPES 4.0 version customized software.

4.4 Competitive immunosensor optimization

4.4.1 Experimental design

The tests for the optimization of the experimental conditions were planned by performing the experiments provided by a two-factors and 3-levels experimental design (number of experiment = 3^2), in order to optimize the concentration of the solutions used for the immobilization of p53 on CNT/GNP-SPCEs and anti-p53 antibody in competition, as also discussed in chapter ***Results and Discussion***.

3 concentration levels were tested for each factor as described in the following table:

Concentration of p53 solution for functionalization of CNT-GNP-SPCEs (Factor A)	
Level	Concentration
-1	0.1 μg/mL
0	1 μg/mL
+1	10 μg/mL
Concentration of anti-p53 antibody in competition (Factor B)	
Level	Concentration
-1	0.5 μg/mL
0	5 μg/mL
+1	50 μg/mL

The concentration for the p53 in competition and for the secondary antibody are mantained costants at 10 μg/mL and 1 μg/mL respectively.

The matrix of the experiments is shown below:

Experiment	Factor	
	Concentration of p53 solution for functionalization of CNT-GNP-SPCEs (A)	**Concentration of anti-p53 antibody in competition (B)**
1	-1	-1
2	0	-1
3	+1	-1
4	-1	0
5	0	0
6	+1	0
7	-1	+1
8	0	+1
9	+1	+1

The experiments were carried out under randomized order.

4.4.2 Processing of experimental data

Once executed these experiments, the main effects of the factors and their interactions were evaluated, by 2-way analysys of variance (ANOVA) performed with the Statgraphics Centurion XV statistical software.

For each experiment an immunocompetition signal was acquired an normalized by the zero signal obtained in then absence of p53 in competition (only DO-7 antibody) in order to evaluate the percent inhibition rate ($S\text{-}S_0/S_0$) for each experimental condition, were S is the signal obtained in the presence of the p53 in immunocompetition and S_0 is the blank signal obtained in the absence of p53 (DO-7 only).

In detail, data were then processed by 2-way ANOVA with interactions, evaluating the significance of the factors A and B and their interaction AB. The target response to be maximized it was the percent inhibition rate.

Moreover, by the Interaction Plot, it is possible to observe the trend of the inhibition rate as a function of a single factor, when the other is fixed.

The optimal experimental conditions are determined by identifying the highest point of the response function, in terms of inhibition rate.

4.5 Competitive immunosensor validation

Validation of sensing device was performed according to the Eurachem guidelines[82] on p53-spiked synthetic urine, used as blank matrix. The detection (LOD) and quantitation (LOQ) limits were assessed as the concentration of analyte giving a signal that is $(3 \cdot s_b)/\sqrt{n}$ and $(10 \cdot s_b)/\sqrt{n}$ above the mean blank signal, respectively, where sb is the standard deviation of the blank signal obtained from ten independent blank measurements and n is the number of replicate measurements for each concentration level explored in the inhibition curve. At least three replicate measurements (independent immunoassays carried out with different p53-modified CNT-GNP-SPCEs on the same extract) were carried out for all standards and samples.

4.5.1 Colorimetric competitive immunoassay (ELISA) set-up

The immunosensor was compared with an “home made", Colorimetric immunoassay (ELISA) " by applying the same protocol tranferred on 96-well plates, since a commercial competitive immunoassay kit for the detection of p53 protein it is not available.

- **p53 protein immobilization**

  Recombinant human p53 protein was immobilized on uncoated 96-well microplate, by overnight incubation at 4°C of a 5 μg/mL solution in bicarbonate buffer (50 μl/well).

- **Blocking**

  After removal of unbound p53 by washings with PBS-T (×3) and PBS (×2), the wells were incubated for 1 h at room temperature with 20 mg/mL BSA in PBS (200 μl/well) as blocking treatment aimed to prevent nonspecific immunoreactivity.

- **Immunocompetition**

  Wells were then washed with PBS (×3) and incubated under shaking for 1 h at RT with 100 μl of the immunocompetition mixture (p53 and anti-p53), analogously to the protocol previously described in the section 2.2.

- **“Reading antibody” incubation**

  After washing with TRIS-T (×3) and TRIS (×2), the wells were incubated for two hours at RT with 100 μl RAM-AP secondary antibody, 10.000-fold diluted in TRIS.

- **Reading of the immunoassay**

  The wells were finally washed with TRIS-T (×3) and with TRIS (×2), and filled with 200 μl of ready to use PNPP solution and the enzyme substrate was allowed to react for 30 minutes. The reaction was stopped with 2.5 M sodium hydroxide and absorbance values were recorded at 405 nm using a Biochrom EZ Read 400 Microplate Reader. Response curves were obtained normalizing the absorbance values observed for each concentration (A) as a function of the signal from zero level (A0) obtained without p53 in competition, analogously to the current data from electrochemical immunoassay.

Results and discussion

The purpose of the present work was the development of an innovative diagnostic system based on immunoenzimatic approach, as clinical evidence of bladder cancer.
The development of the immuno-device involves:

1. The identification of the most appropriate transduction method;
2. The Identification of appropriate strategies for the immobilization of the bioreceptor on the sensor;
3. The identification of the more suitable methodology to detect and quantify the target protein;
4. Optimization of the experimental conditions for the device development and immunoassay setup;
5. Validation of the method in real samples of clinical interest.

Concerning the first two points, we have chosen electrochemical immunosensors with amperometric transduction, since they are considered the most consolidated and effective technique from a biological point of view. Amperometric biosensor are compatible with , low cost, disposable and miniaturized instrumentation, specially designed to work with micro-volume sample, such as the "Screen-Printed Carbon Electrodes" (SPCEs).
Furthermore, a crucial aspect for the realization of an effective immunosensor is the immobilization strategy for the active bioreceptor on the electrodic surface. We chose SPCEs with working electrode functionalized with nanocomposite materials. Specifically, the studied immunodevice was implemented on Carbon nanotubes/Gold Nanoparticles Screen Printed Carbon Electrodes (CNT-GNP SPCEs). This substrate allows the direct chemosorption of the bioreceptor *via* thiol-gold interactions ascribable to the cysteine moieties of the protein, while the active role of carbon nanotubes is exploited in terms of enhancement of the active surface, as well as improvement of the electron transfer process.

Regarding the thirth point, in a first stage of the project we approached a noncompetitive sandwich methodology for the development of the immunosensor. Such methodology evidenced a series of critical aspects, so, also considering that sandwich immunosensors for p53 determination have been challenged in already published works, we focused our attention on a more innovative competitive approach, not reported on literature, concerning p53 as target antigen.

1. Sandwich approach

1.1 First development of the sandwich immunosensor

The immunosensor designed can be represented by the following Figure:

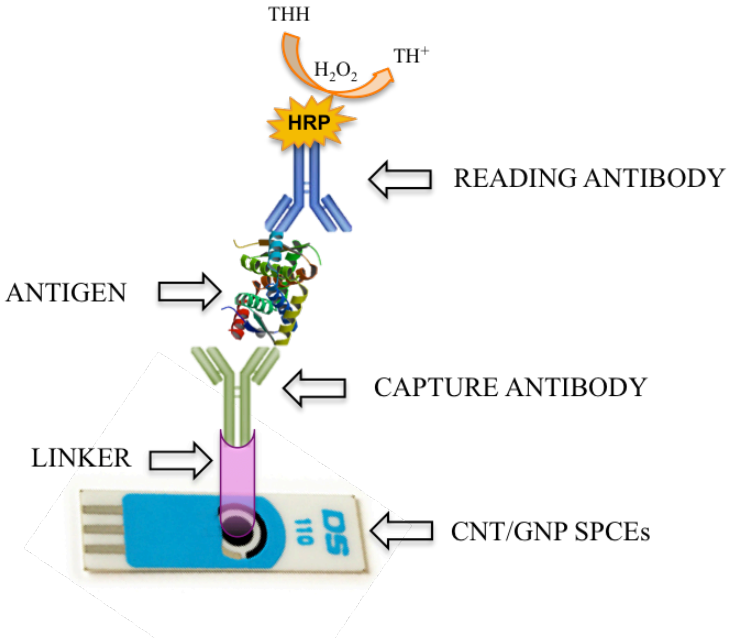

Figure 1: Schematic representation of the operating principle of the sandwich immunosensor.

I. Immobilization of the "capture" antibody with Protein A

Since antibodies are sometimes directly adsorbed on the surface of nanogold, in order to ensure a proper orientation of the immobilized antibody we chosen the Protein A as a linker, because it is able to bind the antibody involving only his Fc region, leaving Fab moiety available for specific interactions with the antigen[83].

II. Cross-linking

The cross-linking procedure, performed with the homobifunctional crosslinker DMP (Figure 2), was used to associate a covalent network to the weak interaction occurring between PA and catching antibody. Moreover, it ensures the stability of the active substrate during the washing after the incubation of the sample and during measurements over the time.

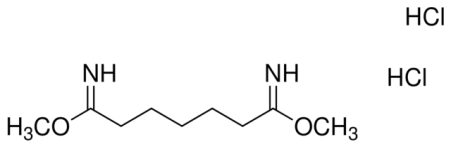

Figure 2: Chemical structure of the crosslinking reagent Dimethyl pimelimidate (DMP) dihydrochloride.

III. Quenching

In order to limit the non-specific interactions, it is then necessary that the coupling reaction is quenched. For this purpose, the quenching solution at pH 7.5, containing the TRIS-HCl was used. The active sites of DMP are blocked by reaction with the primary amino groups of the TRIS-HCl (Figure 3).

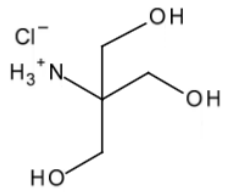

Figure 3: Structural formula of TRIS-HCl

IV. Blocking

Finally, a blocking with BSA is carried out, in order to prevent non-specific responses during the sample incubation.

V. p53 incubation

The functionalized electrode is ready for the step of incubation with the analyte, during which the capture anti-p53 antibody reacts specifically with the protein. The concentration levels explored for p53 were between 0.1 μg/mL and 10 μg/mL.

VI. Incubation of the "reading" antibody

The immunosorbed p53 was attempted to be detected with a "reading" antibody (DO-7 clone) directed toward a different epitope of the analyte

This antibody is labeled with the HRP enzyme, which acts as a label for the analyte determination.

VII. Reading of the electrochemical immunoassay

Therefore, for reading out the immunoassay, it is necessary to use a redox mediator, able to originate a signal related to the concentration of the enzyme immobilized on the electrode surface, through an electrocatalytic cycle, which takes place in the presence of a suitable substrate and which can be schematized as follows:

Enzyme-Substrate reaction $S_O + E_R \rightleftarrows S_R + E_O$

Enzyme-Mediator reaction $E_O + M_R \rightleftarrows E_R + M_O$

Electrodic reaction $M_O + e^- \rightleftarrows M_R$

S_O : oxidized substrate

S_R : reduced substrate

E_R : reduced enzyme

E_O : oxidized enzyme

M_R : reduced mediator

M_O : oxidized mediator

To ensure that this happens two conditions must exist:

$$E^0_{M_O/M_R} > E^0_{E_O/E_R}$$

$$\eta_{M_R/M_O} < \eta_{E_R/E_O}$$

where E^0 is the standard reduction potential and η is the overvoltage to be applied for the oxidation. The first condition ensures that the redox reaction between the enzyme and the mediator is favored thermodynamically. The second condition, instead, is the one that causes that the electrodic process to monitor is the redox reaction dependent from the mediator, because it occurs at lower potentials than those required by the enzyme, with the ability to more easily obtain a signal analytically useful.

In this case, in particular, H_2O_2 and thionine were used as substrate and as redox mediator, respectively:

Enzyme-Substrate reaction $H_2O_2 + HRP(red) \rightleftarrows H_2O + HRP(ox)$

Enzyme-Mediator reaction $HRP(ox) + THH \rightleftarrows HRP(red) + TH^+$

Electrodic reaction $TH^+ + H^+ + 2e^- \rightleftarrows THH$

Hydrogen peroxide initially reacts with the reduced form of peroxidase (HRP-red) generating H_2O and oxidized peroxidase (HRP-ox). Subsequently, cationic thionin (TH^+) is electrochemically reduced to neutral thionin (THH) by reversible bi-electronic mechanism. Finally, HRP-ox reacts with THH generating HRP-red and TH^+ [84].

In the absence of the enzyme substrate, only the electrodic process ascribable to the mediator is observed, giving a signal typical of an electrochemically reversible system. (Figure 4).

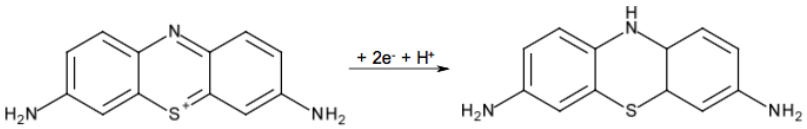

Figure 4: electrodic reaction ascribable to the reduction of the mediator (TH^+ → THH)

Upon addition of H_2O_2 (substrate), the enzymatic mechanism is triggered, with a consequent increase in the concentration of thionine in oxidized form in solution, thanks to the greater contribution of the enzyme-mediator reaction. This results in an increase of cathodic current, with respect to the peak recorded in the absence of the substrate. In detail, it is observed a Peroxide-Induced Current Shift (PICS)[85-87], which represents the analytical signal referable to the concentration of the HRP enzyme immobilized on the electrode surface and, consequently, to the concentration of the target protein p53(Figure 5).

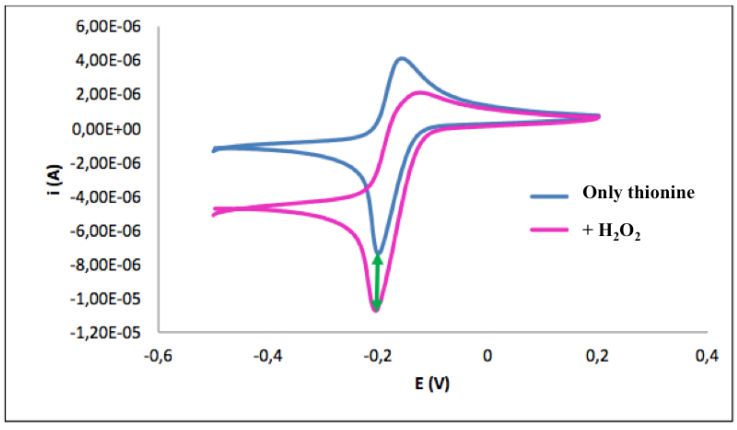

Figure 5: Voltammograms recorded by CV first (blue) and after (magenta) the addition of H_2O_2. The arrow indicates the PICS.

According to the above-decribed protocol we not observed significantly different PICS obtained with increasing concentrations of incubated p53, also including the blank experiments (no p53). In

fact, high PICS values were non-specifically observed.

These findings were interpreted considering that the two anti-p53 antibodies selected (DO-1 and DO-7) recognize two different epitopes of the p53 protein, but this epitopes are contiguous, as confirmed by the antibodies datasheet, so probably affecting the binding of the reading antibody from a conformational point of view.

Moreover, it is important to consider also that HRP-labelled antibodies are not fully compatible with the reading of the assay using thionine as redox mediator. In fact, the reaction mechanism can be influenced by the dissolved oxygen, that is usually stripped out with nitrogen bubbling (purging), when using conventional three-electrodes cells. Since purging with nitrogen is not applicable to SPEs, we decided to switch to Alkaline Phosphatase (AP) conjugated systems, suiting a reading reaction not influenced by dissolved oxygen and, consequently, not requiring the purging step.

1.1.1 Replacement of the HRP enzyme with AP

Before to investigate the possible hindrance problems determined by the proximity of the epitopes, we decided to change the enzyme of reaction in order to overcome the problem of the *purging*. A very interesting enzyme which worked better for us was the alkaline phosphatase, which in the presence of hydroquinone diphosphate (HQDP), not electroactive, generates the electrochemically active hydroquinone as enzyme-assisted dephosphorylation product (Figure 6).

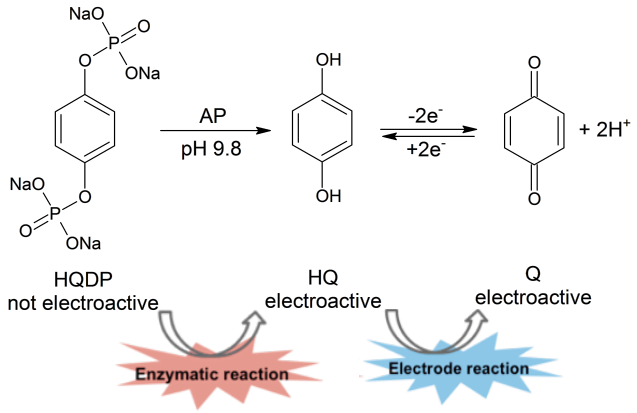

Figure 6: Enzymatic reaction of HQDP.

Even voltammetric readings are easier and immediate (Figure 7).

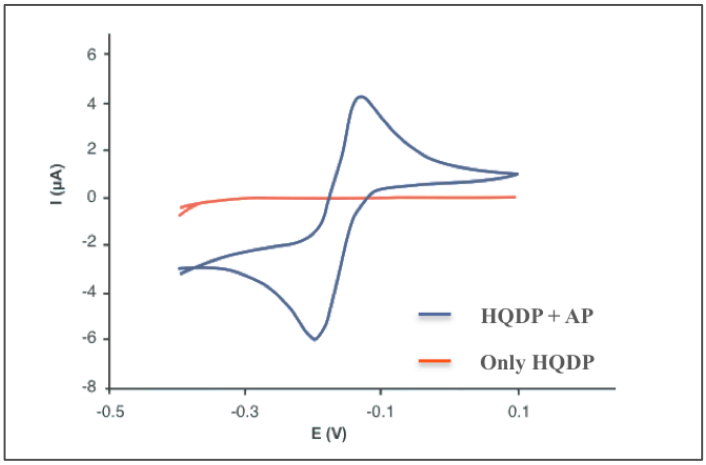

Figure 7: Voltammograms recorded in CV in absence (orange) and in presence (blue) of alkaline phosphatase.

1.2 Second development of the sandwich immunosensor

The protocol is similar to the previous approach, except for the last three steps, as follows:

I. **Immobilization of the "capture" antibody with Protein A**
II. **Cross-linking**
III. **Quenching**
IV. **Blocking**
V. **p53 incubation**

VI. **Incubation of the "secondary" antibody**

In this case the DO-7 antibody was not enzyme-conjugated, so requiring the use of a "reading" anti-antibody.

VII. **Incubation of the "reading" anti-antibody**

Immunosorbed DO-7 was recognized by maeans of an Alkaline Phosphatase-conjugated Rabbit Anti-Mouse IgG (RAM-AP).

VIII. Electrochemical measurements

Non-electroactive HQDP was used as enzyme substrate, since alkaline phosphatase (AP)-promoted dephosphorylation yields electroactive hydroquinone (HQ) that is in turn oxidized to quinone (Q) giving the p53-related analytical signal.

The resulting signals have reconfirmed the absence of significant differences between the various concentrations of p53 incubated and also towards the blanks. Once again all the signals were positives (Figure 8), so indicating the occurrence of aspecific binding of RAM-AP, not related to the formation of the immuno-sandwich. These findings definitevly confirm the unsuitability of the couple DO-1/DO-7 as immunoreagents for sandwich-type assay.

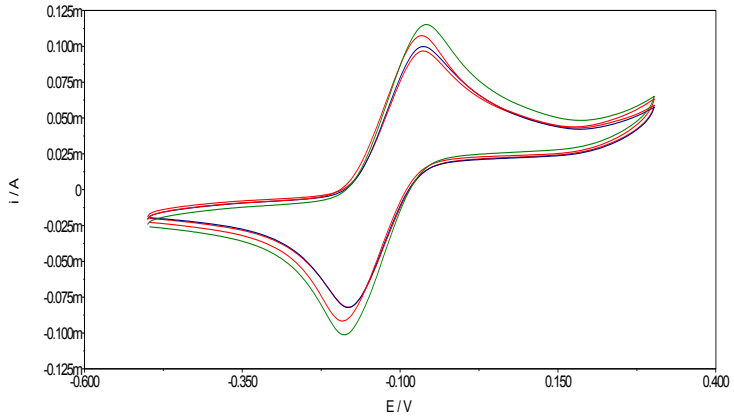

Figure 8: Cyclic voltammetry responses obtained analysing different concentrations of p53 standard solutions. No significant differences related to p53 concentration are observed.

1.3 QCM measurements

In order to further investigate the experimental origin of the unsuccessfully sandwich approach , we studied step by step the binding of the various components, in order to check our hypothesis of affinity and aspecificity. To this purpose, parallel experiment on QCM (Quartz Crystal Microbalance, Figure 9) sensors were performed.

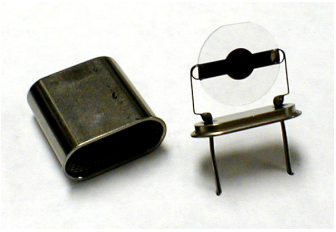

Figure 9: Quartz crystal microbalance

In detail, the QCM equipements are mass sensors, whose operation is based on the piezoelectric properties of quartz. In particular, if subjected to an alternating potential, the piezoelectric quartz vibrate at a characteristic oscillation frequency, which undergoes variations as a function of its mass. If the quartz is covered by a gold layer, they are also called frequentiometric sensors, because it is possible to measure a decrease of frequency that is directly proportional to the increase of mass, due to the immobilization of the analyte of interest on them, according with the Sauerbrey equation (1):

$$\Delta f = -\frac{2f_0^2}{A\sqrt{\rho_q \mu_q}}\Delta m \qquad (1)$$

f_0 = Fundamental Resonance frequency (Hz)
Δf = Frequency change (Hz)
Δm = Mass change (g)
A = Piezoelectrically active crystal area
ρ_q = Density of quartz
μ_q = Shear modulus of quartz for AT-cut crystal

In this way, it is possible to monitor online the binding/sorption phenomena occurring at the solution/gold interface[88].

1.3.1 QCM modification

Prior to functionalization, each quartz crystal was appropriatly cleaned and activated as follows: it was sonicated in 2-propanol for 3 min, then immersed in 1.2 M NaOH for 10 min and in 1.2 M HCl for 5 min. The rinsed crystal was mounted in a QCM off-line cell in order to perform the subsequent treatments only on the selected gold surface. This gold surface was exposed to a drop of concentrated HCl (37 %, v/v) for 30 s, rinsed with deionized water again and finally washed with ethanol for three times to be thus assembled in a flow cell. First the crystal was washed with deionized water and then the PBS 1x was fluxed for 3 min. The electrode was finally kept under static conditions for further 3 min in order to get a stable baseline signal. The subsequent functionalization has followed the steps of the protocol described for the sandwich analytical immunosensor.

The frequency change (Df [Hz]) was estimated as difference between the final baseline frequency, evaluated at the end of the washing steps in static mode, and the frequency of washing buffers steady-state step just before incubation of the different components.

The recorded sensorgram is shown in Figure 10.

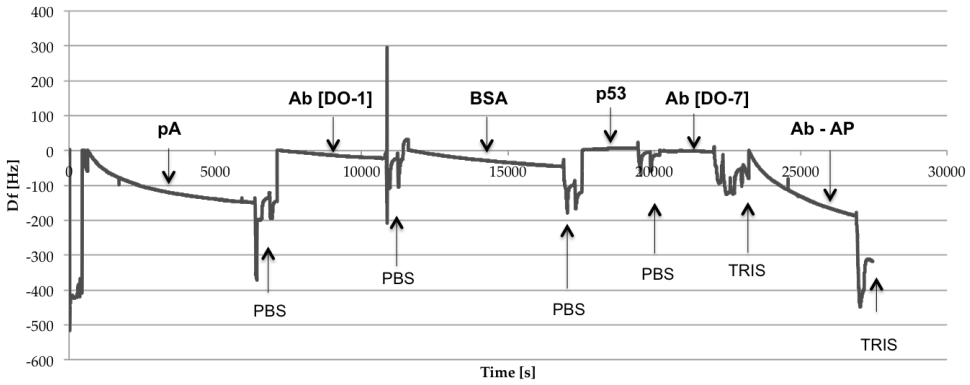

Figure 10: Sensorgram (frequency vs time) of the parallel experiment conducted on QCM.

As showed in the frequencygram reported in figure 10, frequency changes (decreases) were observed upun incubation of PA and, more slightly, of DO-1, so evidencing the strong chemisorption of PA and a following immobilization of the capture antibody. Blocking with BSA also results in a expected mass increase (frequency decrease). When the p53 protein is incubated no changes in frequency are observed, evidencing that the protein is not bound to its capture antibody, under these conditions. This could mean with good probability that the protein A does not show a so strong affinity for the Fc portion of DO-1, which can be so linked also via the Fab portion, which will not result free and correctly orientated to bind the p53 target protein.

The findings of the QCM measurements not only agree with the results of amperometric exeperiments, but also give a possible explaination about the cause of the problem. A possible solution could have been identified in the replacement of the Fc binding protein, switching, for example to protein G, or to other linker molecules. Hovewer, also considering the practical advantages in terms of costs and time involved in the competitive assay, we decide to move our efforts on a competitive immunosensor, also considering the novelty of this approach, not yet published for p53.

2. Competitive approach

2.1 Preliminary test for the affinity of p53

The competitive immunosensor designed can be represented by the following scheme:

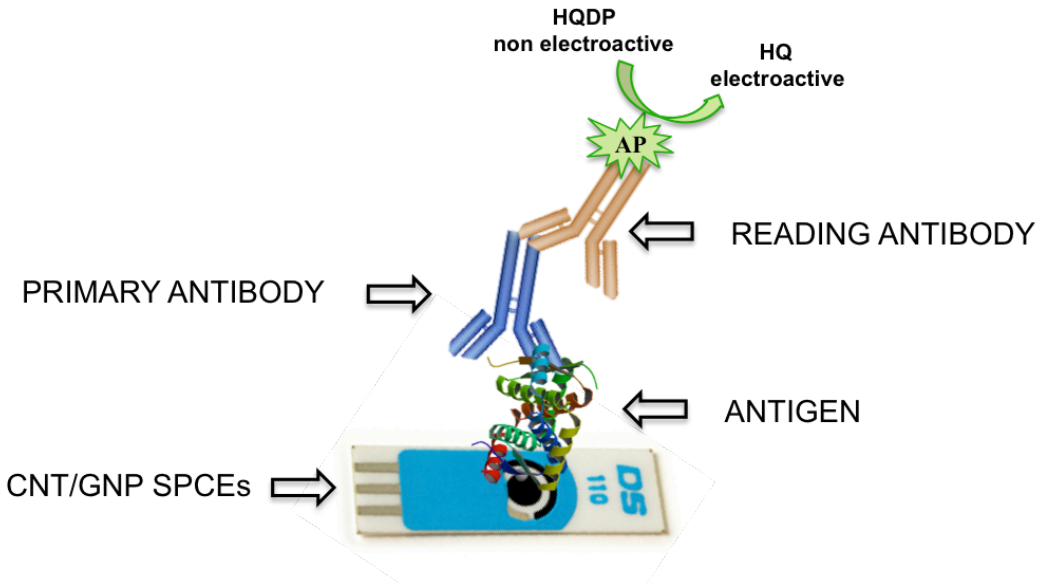

Figure 11: Schematic representation of the operating principle of the competitive immunosensor.

A crucial aspect for the realization of an effective immunosensor is the proper immobilization of the active bioreceptor on the electrodic surface. The use of carbon nanotubes/gold nanoparticles composite as electrodic substrate allows the direct chemisorption of p53 via thiol-gold interactions ascribable to the cysteine moieties of the protein, while the active role of carbon nanotubes is exploited in terms of enhancement of the active surface. In the specific case of competitive immunosensor, the target antigen protein has to be bound in such a way as not to involve the functional groups of the immuno-active epitope, in order to preserve the reactivity with the specific antibody used for the immunocompetition. For this purpose, before to conduce the competition experiments, immobilized p53 versus anti-p53 "titrations" were carried out, in order to check the effective immobilization of p53 and to identify the experimental dynamic domain for the subsequent optimization of the immunocompetition. A first set of experiments was therefore performed fixing at 10 μg/mL the concentration of the p53 solution used for functionalization of the CNT/GNP-SPCEs and incubating the so obtained electrodes firstly with solutions of anti-p53 ranging from 0 (no antibody) to 50 μg/mL and subsequently with RAM-AP secondary antibody. Analogous experiments were performed varying the concentration of the p53 solution used for

functionalization of the CNT/GNP-SPCEs from zero to 10 μg/mL and keeping constant the concentration of anti-p53 at 50 μg/mL. In both cases, our findings evidenced CV signals increasing versus anti-p53 and p53 concentration, respectively. Very weak background signals were recorded in the absence of both anti-p53 and p53, evidencing the proper immobilization of the bioreceptor as well as the non-occurrence of nonspecific binding phenomena (Figure 12).

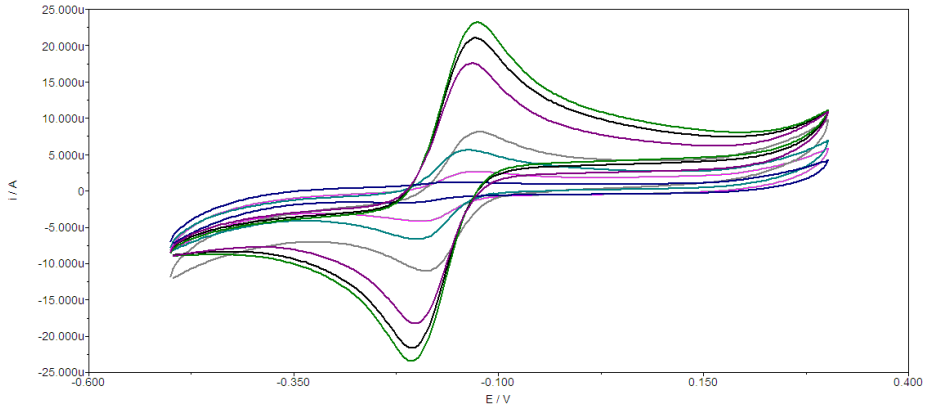

Figure 12: Example of signal increase with increasing of anti-p53 Ab concentration and very weak background signal in the absence of anti-p53 (blue signal).

On the basis of these results, the optimal concentrations of *i)* immobilized p53 and *ii)* anti-p53 antibody were assessed by means of two-factors and 3-levels experimental design procedure.

2.2 Optimization of the immunocompetition

The experimental design was aimed at finding the optimal condition leading to highest signal inhibition for a p53 concentration in competition fixed at 10 μg/mL.

For this purpose, the explored concentration levels (as also discussed in chapter ***Matherial and Methods***) were 0.1, 1 and 10 μg/mL for the solution used for the immobilization of p53 on the CNT/GNP-SPCEs, while anti-p53 antibody concentration levels were 0.5, 5 and 50 μg/mL. Two-way ANOVA results show that both factors (p53 and anti-p53) and their interaction have a significant effect (*p-value <0.05*) on the immunosensor response (Figure 13), with optimal concentrations for p53 and antibody of 1 μg/ml and 5 μg/ml respectively, leading to maximized inhibition rate.

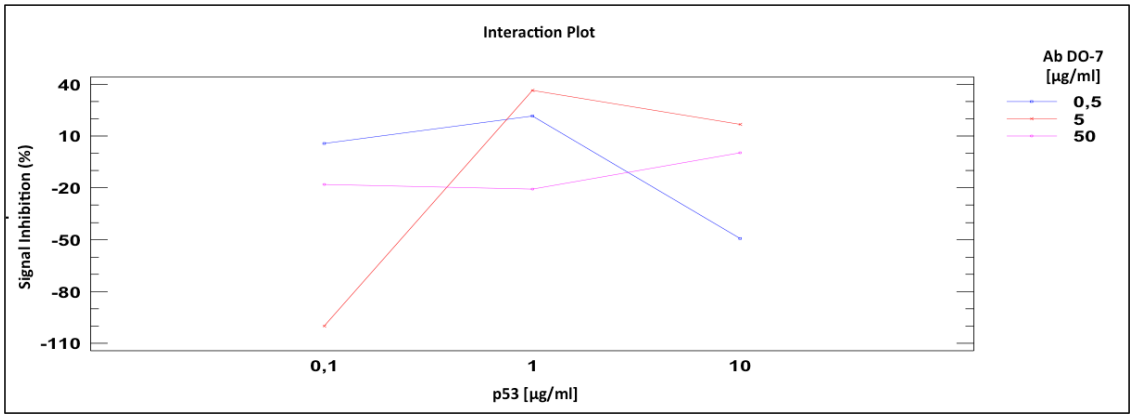

Figure 13: Interaction plot from ANOVA, evidencing the effects of anti-p53 Ab and p53 concentrations on the signal inhibition extent.

On the basis of these results, the explored experimental domain was narrowed over the 0.5 - 5 µg/ml and 2.5 - 10 µg/ml concentration ranges for p53 and anti-p53, respectively, and a second ANOVA was carried out (Figure 14). Modulating these variables, we have found out so the optimal experimental conditions leading to highest signal inhibition associated to the increase of the p53 concentration present in the sample. According to the obtained results, the p53 concentration for the functionalization of GNP-SPCEs was fixed at 5 µg/ml, while the optimal concentration of anti-p53 resulted to be 2.5 µg/ml.

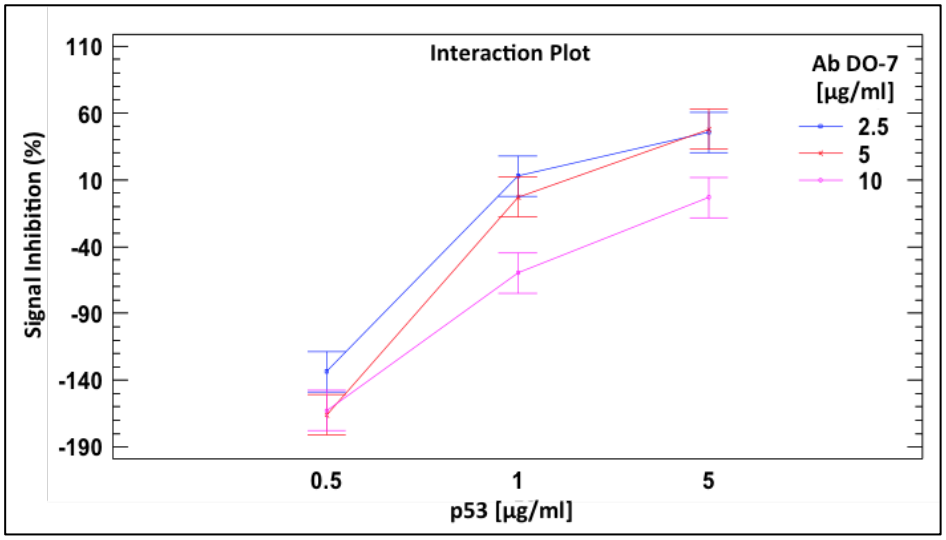

Figure 14: Interaction plot from ANOVA in the narrowed experimental domain, evidencing the effects of anti-p53 Ab and p53 concentrations on the signal inhibition extent.

2.3 Immunosensor setup

As decribed in chapter ***Matherial and Methods*** the competitive protocol includes the following steps, as show in Figure 15:

I. **Chemosorbtion of p53**
II. **Blocking**
III. **Competition**
IV. **Incubation of the "reading" antibody**
V. **Electrochemical measurements**

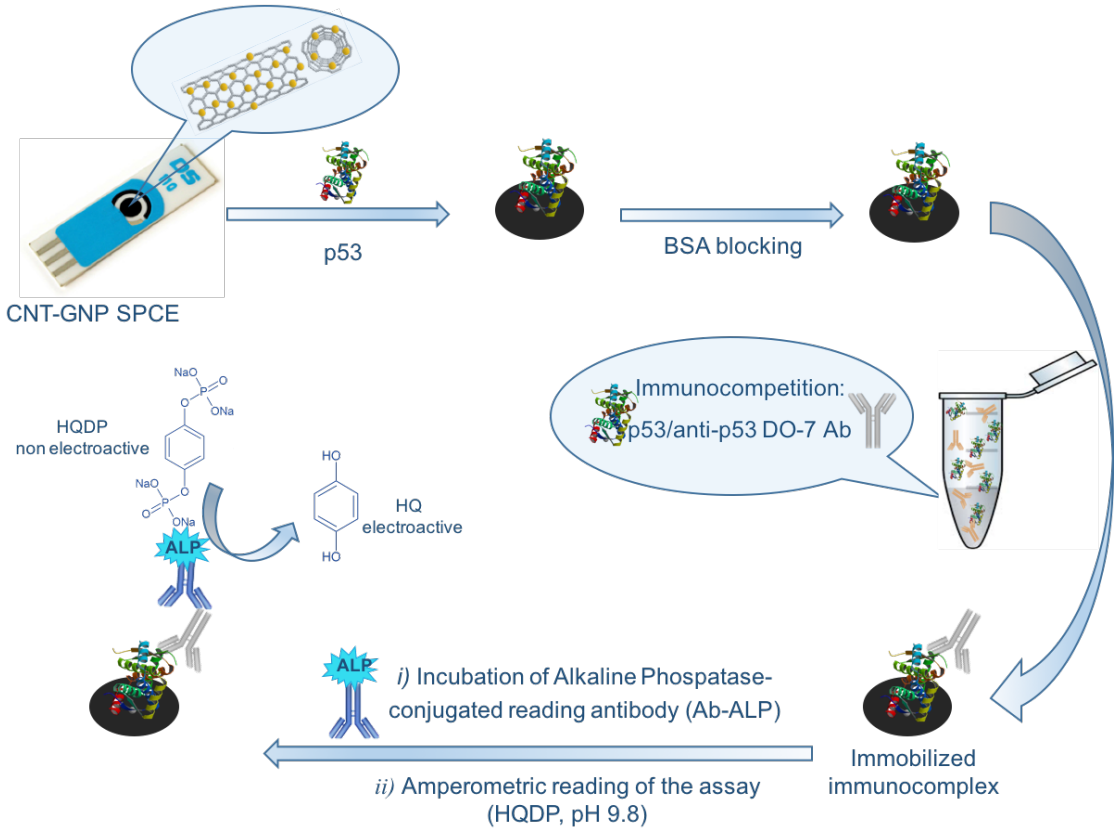

Figure 15: Schematic representation of the fabrication protocol of the competitive immunosensor and set-up of the immunoassay implemented on disposable Carbon Nanotubes/Gold Nanoparticles- Screen-Printed Carbon Electrodes.

After the optimization of the competitive device , the readings of the assays were performed using differential pulse voltammetry (DPV). This electrochemical detection is more useful for analytical purposes, unlike the CV that is more properly an exploratory technique. It is caracterized by a well-shaped peak, a reduced background signal (capacitive), an enhanced analytical signal (faradic) and a signal/noise ratio improvement (better sensitivity).

In this case, is effectuated a normalization of the current values observed for each concentration of p53 (S) as a function of the signal from zero level (S_0) obtained without p53 in competition, and the normalized signals are expressed as percentage values (S/S_0 x 100). Because the ability of p53 in competition is to inhibit antibody binding to the immobilized protein, increasing analyte concentration will reduce the amount of anti-p53 bound to the modified immunosensor surface and the signal observed will be inversely proportional to the concentration of the analyte of interest (Figure 16).

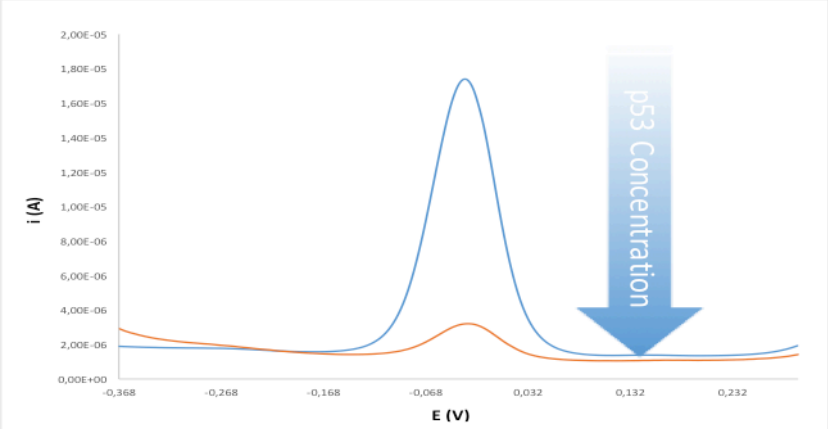

Figure 16: % inhibition rate (S/S_0 x 100), referred to the blank signal (no p53 in competition)

2.4 Immunosensor performance

The analytical performance of the immunosensor was assessed under the optimized experimental conditions carryng out competitive assay firstly on standard solution of p53, prepared in PBS. Figure 17 shows DPV scans recorded over the 0 – 10 nM concentration range.

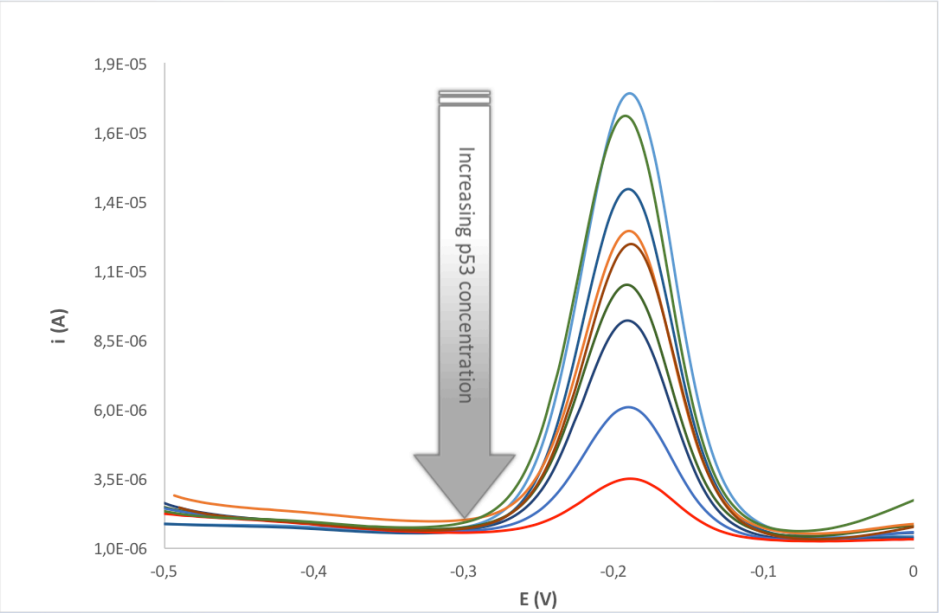

Figure 17: Selection of DPV scans recorded over the 0-10 nM p53 concentration range.

The inhibition response curves were obtained plotting the normalized signals, expressed as percentage values (S/S_0 x100), versus the logarithm of the p53 concentration and fitted using a four-parameter logistic function (2), as conventional for competitive immunoassay[89,90] (figure 18).

$$S/S_0 = S_{min} + \frac{(S_{max} - S_{min})}{1 + ([C]/I_{50})^B} \qquad (2)$$

where S_{min} and S_{max} are the asymptotic minimum and maximum, respectively (S_{max} is recorded in the absence of analyte), and B is the curve slope at the inflection point I_{50}, corresponding to the p53 concentration (C) giving 50 % of signal inhibition. Data fitting was performed using the software product Microcalc OriginPro 8.5.

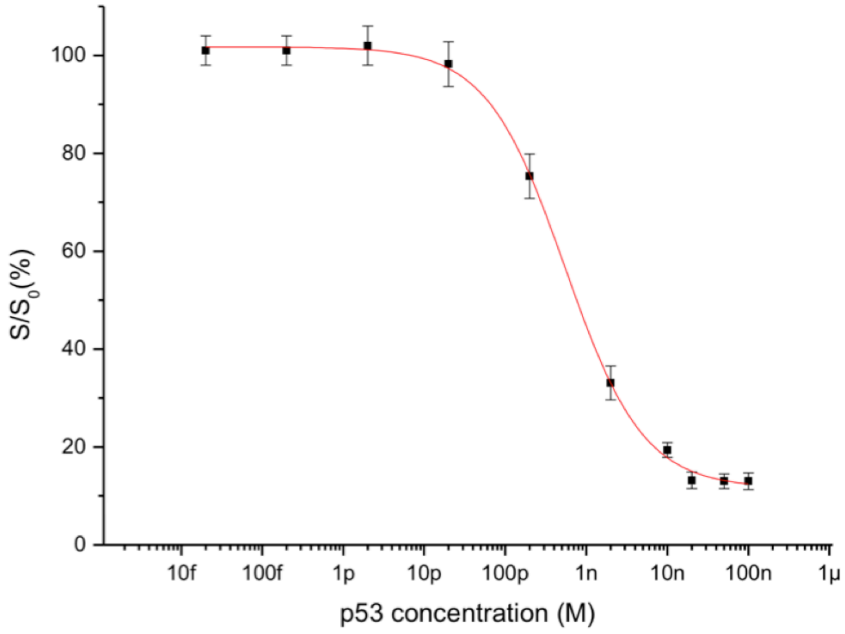

Figure 18: Inhibition curve obtained interpolating the dataset from analysis of different p53 standard solution. *Inset table*: fitted curve parameters.

Under optimized conditions, the developed immunosensor showed very good analytical performance in terms of sensitivity, precision and trueness. LOD and LOQ values of 35 and 123 pM, respectively, were calculated. A comparison with the performance obtained with other electrochemical biosensors, based on sandwich immunochemical approach and requiring very complex and time/cost-expensive nanostructures, is reported below, in Table 1.

Table 1: Comparison of the performance of our competitive immunosensor with other amperometric immunosensor for determination of wild type or mutated p53, mainly involving multi-nanostructured architectures.

Analytical approach	**Target p53**	**Declared LOD**	**Linear range**	**Reference**
Sandwich /graphene /chitosan substrate	Phospho-p53[15]	100 pM	0.2-10 nM	Xie et al, 2011
Sandwich/Graphene Oxide-Conjugate Antibodies	Phospho-p53[392]	10 pM	0.2-2 nM	Du et al, 2011
Sandwich/Magnetic Beads/ enzyme-conjugate carbon nanosphere	Phospho-p53[392]	3.3 pg mL^{-1}	0.01-5 ng mL^{-1}	Luo et al, 2014
Sandwich/ Graphene	Wildtype p53	0.03 pM	0.2-2 pM	Afsharan

Oxide/Gold nanoparticles-streptavidin conjugate				et al, 2016
Competitive assay on p53-modified gold nanoparticles/carbon nanotubes screen-printed electrodes (no nano-conjugated used)	Wildtype p53[a]	14 pM	20pM-10nM	**Present work**

a) DO-7 Antibody is able to recognize both wildtype and mutated p53

2.5 Immunosensor validation

Thus established that the system works properly and with good results, it has been successfully validated in untreated and undiluted Synthetic Urine spiked with p53, as a biological matrix. We obtained a dynamic range of response between 10 pM and 10 nM comparable to those obtained in physiological buffer, in terms of concentration values of p53 in competition (Figure 19). The LOD and LOQ values calculated in synthetic urine were of 35 and 123 pM respectively, not significantly different from those obtained in physiological buffer, so evidencing the excellent performance of the sensor, not showing significant matrix effect from synthetic urine.

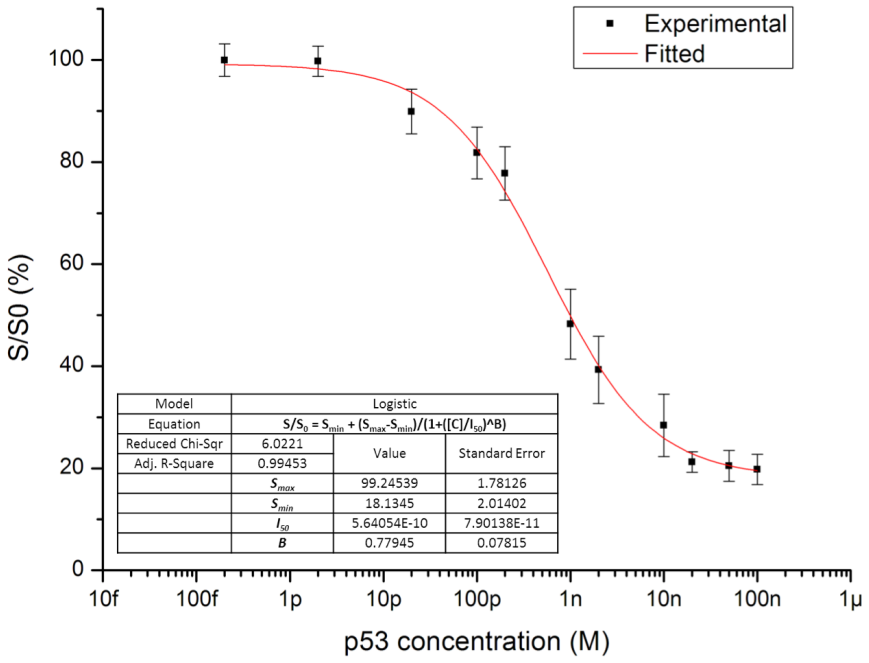

Figure 19: Inhibition curve for p53-spiked undiluted Synthetic Urine, obtained interpolating the dataset from immunocompetition experiments carried out on p53-modified CNT/GNP-SPCEs. Inset table: fitted curve parameters.

Concerning precision, relative standard deviation (RSD) always lower than 10% (n = 3) were observed over the explored concentration range. Trueness was assessed analysing standard solutions not included in the calibration dataset, giving the recovery rates reported in Table 2.

Table 2. Trueness of the competitive immunosensor, assessed analysing p53-spiked Synthetic Urine and calculating % recovery rates as (found value /spiked value x 100).

Spiked p53 (in Synthetic Urine)	Found p53[a]	% Recovery Rate
100 pM	124 ± 10 pM	124 ± 10
1 nM	0.912 ± 0.073 nM	91 ± 7
10 nM	13.2 ± 1.2 nM	132 ± 12

a) analysed with p53-modified *CNT/GNP-SPCEs and interpolated according to the inhibition curve reported in Figure 19*

The performance of the competitive immunosensor were also compared with the findings from conventional ELISA immunochemical competitive assays, developed by us as described in section 4.4.1 of chapter ***Matherial and Methods***. Under the same experimental condition used for the electrochemical immunosensor, the spectrophotometric ELISA method showed worst performance in terms of LOD, LOQ and sensitivity, so highlighting the high potential of our immunosensor, due to the synergic combination of CNT/GNP substrates and amperometric transduction (Figure 20 and Table 3).

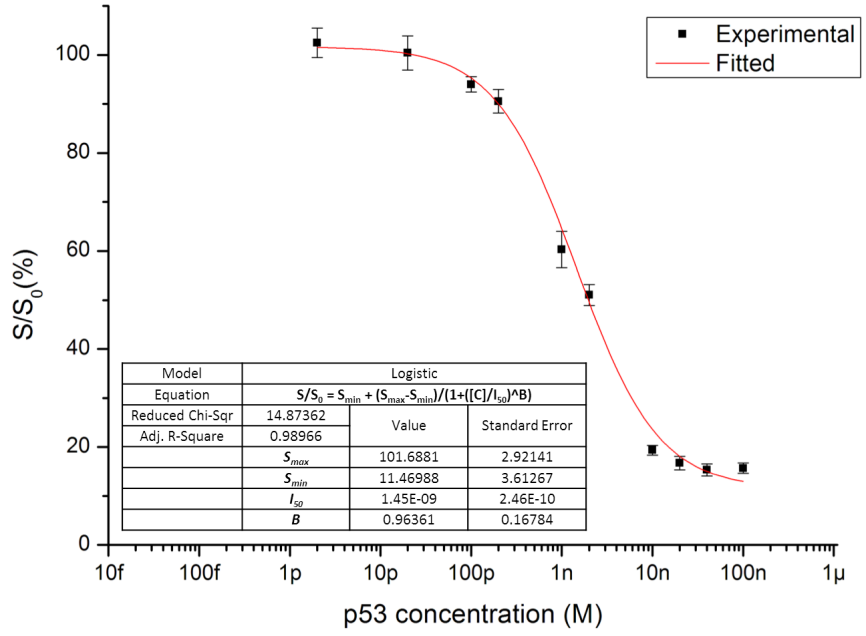

Figure 20: Inhibition curve from home-made spectrophotometric ELISA microtiter plates, obtained interpolating the dataset from analysis of different p53 matrix solution. *Inset table*: fitted curve parameters.

Table 3: Schematic overview of analytical performance of our immunosensor for the detection of p53 in PBS and in Matrix solution. The performances are also compared with those obtained with ELISA approach.

Analytical approach	**Dynamic range**	**LOD**	**LOQ**
Immunosensor working in PBS	20 pM - 10 nM	35	123
Immunosensor working in S-Urine	20 pM – 10 nM	14	100
ELISA working in S-Urine	100 pM – 50 nM	114	380

Conclusions

At the conclusion of this thesis, animated by the aim to design a diagnostic immuno-device to replace the laborious and expensive techniques currently in use, we have developed, to the best of our knowledge, the first competitive amperometric immunosensor for determination of p53 protein.
In order to obtain this objective, the most significant results achieved during the course of this thesis can be summarized as follows.
First of all, we decided to project the new devices with amperometric transduction, because are very versatile tools for rapid and user-friendly screening analysis, thanks to their compatibility with portable and compact devices, exploiting disposable "Screen-Printed" electrodes as sensing substrates. In particular, we implemented the immunosensor on carbon nanotubes-gold nanoparticles screen-printed glassy carbon electrodes (CNT/GNP SPECs), because we experimented that they were the best to maintain unchanged the function of the biological elements. This choice has proved to be optimal because this substrate has improved the sensitivity of the immunosensor thanks to the high active surface for the immobilization of p53. Then, we firstly tried to develop a sandwich format assay. This approach however didn't give us good results, because of unproper orientation problems were evidenced and confirmed both by amperometric measurments and confirmatory QCM experiments, that allowed us to identify the reason of this unsuccesfull approach.
On the basis of these results, also considering the practical advantages in terms of costs and time involved in the competitive assay, we decide to move our efforts on a competitive immunosensor, also considering the novelty of this approach, not yet published for p53.
The competitive immunosensor developed for the first time in this work for determination of the p53 protein was found to be highly promising for detection of the biomarker at subnanomolar levels in urine samples, showing good sensitivity, selectivity and stability. The developed immunosensor has promising perspectives as simple, reliable and analytically robust diagnostic tool, valuable for implementation of screening and follow-up programs for urological malignancies.
On comparing with sandwich immunosensors for p53 determination, involving very complex and time/cost expensive nanostructured architectures, this competitive immunodevice offers performance comparable or even better than those of most of the sandwich immunosensors reported in literature for detection of differently mutant p53 forms.
As the single anti-p53 mouse monoclonal antibody (DO-7 clone) is able to recognize both wild-type and mutant p53, the immunosensor could be efficiently applied to rapid and wide-range pre-screening evaluations, focusing the attention on positive samples for more exhaustive and

meaningful confirmation analyses carried out with biomolecular approaches, in order to discriminate the mutation degree of the target biomarker, also considering the relatively short half-life of this complex protein. Finally, the competitive device could be also proposed for determination of anti-p53 antibodies on the same sensing substrate, by direct incubation of the sample in the absence of experimentally induced immunocompetition, making the immunosensor a very versatile diagnostic tool for widespread application for biomedical purposes.

The results of this study were recently submitted for the publication as “full research paper” on the highly specialistic journal “Biosensors and Bioelectronics” (Elsevier). At the time when this thesis was delivered, the manuscript was in the “under review” status.

References

1. Weinberg R.A, 1988. *Trans Stud Coll Physicians Phila*; 243, 38-46.
2. The best Science of 1992. *Time*; 62.
3. Molecule of the year - p53 sweeps through cancer research, 1993. *Science*; 262, 1958-1959.
4. Bode A.M., Dong Z.G., 2004. *Nat. Rev. Cancer*; 10, 793-805.
5. Lane D.P., Benchimol S., 1990. *Gene & Development*; 4, 1-8.
6. Levine A.J., Momand J., Finlay C.A., 1991. *Nature*; 351, 453-456.
7. Kastan M., 1993. *Journal of NIH Research*; 5, 53-57.
8. Stephens T., 1991. *Journal of NIH Research*; 3, 32-36.
9. Vogelstein B., Kinzler K.W., 1992. *Cell*; 70, 523-526.
10. Lane D.P., 1992. *Nature*; 358, 15-16.
11. Hinds P., Finlay C., Levine A.J., 1989. *J Virol*; 63, 739-46.
12. Hollstein M., Rice K., Greenblatt M.S., Soussi T., Fuchs R., Sørlie T., Hovig E., Smith-Sørensen B., Montesano R., Harris C.C., 1994. *Nucleic Acids*; 22, 3551-3555.
13. Chen J., Lin J., Levine A.J., 1995. *Mol. Med*; 1, 142-152.
14. Zhao K., Chai X., Johnston K., Clements A., Marmorstein R., 2001. *J. Biol. Chem*; 276, 12120-12127.
15. Pavletich N.P., Chambers K.A., Pabo C.O., 1993. *Genes Dev*; 7, 2556-2564.
16. Hainaut P., Wiman K.G., (Eds), 2005. *Springer, New York*; 446.
17. Vogelstein B., Lane D., Levine A.J., 2000. *Nature*; 408, 307–310.
18. Vousden K.H., Prives C., 2009. *Cell*; 137, 413–431.
19. Goodsell David S., 2002. *RCSB Protein Data Bank*.
20. Joerger A.C., Fersht A.R., 2010. *Cold Spring Harb Perspect Biol*; 2: a000919.
21. Tidow H., Melero R., Mylonas E., Freund S.M., Grossmann J.G., Carazo J.M., Svergun

D.I., Valle M., Fersht A.R., 2007. *Proc Natl Acad Sci*; 104, 12324-12329.

22. Barak Y., Juven T., Haffner R., Oren M., 1993. *EMBO J*; 12, 461-468.

23. Michael D., Oren M., 2003. *Semin. Cancer Biol*; 13, 49–58.

24. Tan Z.Q., Tu W.L., Schreiber S.S., 2001. *Mol. Brain Res*; 91, 179–188.

25. Davison T.S., Yin P., Nie E., Kay C., Arrowsmith C.H., 1998. *Oncogene*; 17, 651–656.

26. Brown C.J., Lain S., Verma C.S., Fersht A.R., Lane D.P., 2009. *Nat. Rev. Cancer*; 9, 862−873.

27. Shu K.X., Li B., Wu L.X., 2007. *Colloids and Surfaces B: Biointerfaces*; 55, 10 - 18.

28. Tan Z.Q., Tu W.L., Schreiber S.S., 2001. *Mol. Brain Res*; 91, 179-188.

29. Cho Y., Gorina S., Jeffrey P.D., Pavletich N.P., 1994. *Science*; 265, 346 – 355.

30. Friedman P.N., Chen X., Bargonetti, J., Prives C., 1993. *Proc Natl Acad Sci Usa*; 90, 3319-3323.

31. Levine A.J. 1997. *Cell*; 88, 323-331.

32. Toledo F., Krummel K.A., Lee C.J., Liu C.W., Rodewald L.W., Tang M., Wahl G.M., 2006. *Cancer Cell*; 9, 273-285.

33. Malkin D., Li F.P., Strong L.C., Fraumeni J.F. Jr, Nelson C.E., Kim D.H., Kassel J., Gryka M.A., Bischoff F.Z., Tainsky M.A., et al., 1990. *Science*; 250, 1233-1238.

34. Petitjean A., Mathe E., Kato S., Ishioka C., Tavtigian S.V., Hainaut P., Olivier M., 2007. *Hum Mutat*; 28, 622-629.

35. Fontanini G., Fiore L., Bigini D., et al. 1994. *Int J Oncol*; 5:, 553-558.

36. Nag S., Qin J., Srivenugopal K.S., Wang M., Zhang R., 2013. *The Journal of Biomedical Research*; 27, 254-71.

37. Messing E.M., in: Walsh P.C., Retik A.B., Vaughan E.D. Jr, Wein A.J. (Eds), 2002. *Campbell's urology*. 8th ed. Philadelphia: WB Saunders; pp. 2765–2773.

38. Hollstein M., Sidransky D., Vogelstein B., Harris C.C., 1991. *Science*; 253, 49-53.

39. Gopi Kishore M., Hamid A., Dwivedi U.S., et al. 2003. *Uro Oncol*; 2, 121-128.

40. Luo J.C., Neugut A.I., Garbowski G., Forde K.A., Treat M., Smith S., Carney W.P., Brandt-Rauf P.W., 1995. *Cancer Lett*; 91, 235-240.

41. Suwa H., Ohshio G., Okada N., Wang Z., Fukumoto M., Imamura T., Imamura M., 1997. *Gut*; 40, 647-653.

42. Indulski J.A., Lutz W., Krajewska B., 1999. *Cejoem*; 5, 17-25.

43. Lipponen P.K., 1993. *Int J Cancer*; 53, 365-370.

44. Darabi M., Tayebi Meibodi N., Mahdavi R., Arab D., 2006. *Urol J. Fall*; 3, 216-219.

45. Kibel A.S., Nelson J.B., in: Walsh P.C., Retik A.B., Vaughan E.D. Jr, et al, (eds), 2002. *Campbell's urology*. 8th ed. Philadelphia: WB Saunders; p. 2637.

46. Balogh G.A., Mailo D.A., Corte M.M., et al. 2006. *Int J Oncol*; 28, 995-1002.

47. Chong B.E., Lubman D.M., Rosenspire A.J., Miller F.R., 1998. *Rapid Commun. Mass Spectrom*; 12, 1986–1993.

48. O'Toole D., Couvelard A., Rebours V., Zappa M., Hentic O., Hammel P., Levy P., Bedossa P., Raymond E., Ruszniewski P., 2010. *Endocrine-related cancer*; 17, 847.

49. Cox M.L., Meek D.W., 2010. *Cellular signalling*; 22, 564.

50. Domenici F., Bizzarri A.R., Cannistraro S., 2012. *Analytical biochemistry*; 421, 9.

51. Wilson P., Jiang T., Minunni M.E., Turner A.P., Mascini M., 2005. *Biosensors and Bioelectronics*; 20, 2310.

52. Ahmet Koyun, Esma Ahlatcıoğlu and Yeliz Koca İpek, 2012. Prof. Sadik Kara (Ed.). *Biosensors and Their Principles*; 116.

53. Sassolas A., Blum L.J., Leca-Bouvier B.D., 2011. *Biotechnology Advances*; 30, 489-571.

54. Nambiar S., Yeow J.T.W., 2011. *Biosensors and Bioelectronics*; 26, 1825–1832.

55. Thevenot D.R., Toth K., Durst R.A., Wilson G.S., 1999. *Pure Appl. Chem*; 7, 2333-2348.

56. Bradshaw L., 2000. *RF time and frequency*; 8, 50-58.

57. Janshoff A., Galla H.J., Steinem C., Angew. 2000. *Chem. Int. Ed. 39*; 4004- 4032.

58. Bianchi F., Giannetto M., Careri M., 2014. *Anal. Bioanal. Chem*; 406, 15-20.

59. Devi V.R., Doble M., Verma R.S., 2015. *Biosens. Bioelectron*; 68, 688-689.

60. Scouten W.H., Luong J.H.T., Brown R.S., 1995. *Tibtech*; 13, 178-184.

61. Sharma S.K., Sehgal N., Kumar A., 2003. *Current Applied Physics*; 3, 307-316.

62. Dueker R.E., Montague M.T., Leggett G.J., 2008. *Biointerphase 3*; 59-65.

63. Buzea C., Pacheco I.I., Robbie K., 2007. *Biointerphases 4*; MR17-MR71.

64. Luo X., Morrin A., Killard A.J., Smyth M.R., 2006. *Electroanalysis*; 18, 319-326.

65. Siangproh W., Dungchai W., Rattanarat P., Chailapakul O., 2011. *Analytica Chimica Acta*; 690, 10-25.

66. Wang J., 2012. *Microchimica Acta*; 177, 245-270.

67. Daniel M.C., Astruc D., 2004. *Chemical Reviews*; 104, 293-346.

68. Guo S.J., Wang E.K., 2007. *Analytica Chimica Acta*; 598, 181-192.

69. Li Y., Schluesener H.J., Xua S., 2010. *Gold Bulletin*; 43, 29-41.

70. Babacan S., Pivarnik P., Letcher S., Rand A.G., 2000. *Biosens. Bioelectron*; 15, 615-621.

71. Huang C.H., Li J.X., Tang Y., Chen Y.Y., 2011. *Curr. Appl. Phys*; 11, 353-357.

72. Jaroslaava T., 1999. *J. Chromatogr. B Biomed. Sci. Appl*; 722, 11-31.

73. Martin C.R., Mitchell D.T., 1998. *Anal. Chem*; 70, 322-327.

74. Han S.H., Kim S.K., Park K., Yi S.Y., Park H.J., Lyu H.K., Kim M., Chung B.H., 2010. *Analytica Chimica Acta*; 665, 79.

75. Giannetto M., Mattarozzi M., Umiltà E., Manfredi A., Quaglia S., Careri M., 2014. *Biosens Bioelectron*; 62, 325–30.

76. Couto R.A.S., Lima J.L.F.C., Quinaz M.B., 2016.*Talanta*; 146, 801–14.

77. Renedo O.D., Alonso-Lomillo M.A., Martínez M.J., 2007. *Talanta*; 73, 202–19.

78. Xie Y., Chen A., Du D., Lin Y., 2011. *Analytica chimica acta*; 699, 44.

79. Du D., Wang L., Shao Y., Wang J., Engelhard M.H., Lin Y., 2011. *Analytical Chemistry*; 83, 746.

80. Yanan Luo, Abdullah Mohamed Asiri, Xiao Zhang, Guohai Yang, Dan Du, Yuehe Lin, 2014. *RSC Adv*; 4, 54066-54071.

81. Hadi Afsharan, Balal Khalilzadeh, Habib Tajalli, Mahmood Mollabashi, Farzaneh Navaeipour, Mohammad-Reza Rashidi, 2016. *Electrochimica Acta;* 188, 153–164.

82. Magnusson B., Örnemark U. (eds.) Eurachem Guide: The Fitness for Purpose of Analytical Methods – A Laboratory Guide to Method Validation and Related Topics, (2nd ed. 2014). ISBN 978-91-87461-59-0. Available from http://www.eurachem.org".

83. Tang, D., Yuan, R., Chai, Y., 2008. *Anal. Chem*; 80, 1582-1588.

84. Yang M., Yang Y., Yang Y., Shen G., Yu R., 2004. *Anal. Biochem*; 334, 127-134.

85. Giannetto M., Mori L., Mori G., Careri M., Mangia A., 2011. *Sensors & Actuators B*; 159, 185-192

86. Giannetto M., Maiolini E., Ferri E.N., Girotti S., Mori G., Careri M., 2013. *Analical and Bioanalytical Chemistry*; 405, 737-743.

87. Giannetto M., Elviri L., Careri M., Mangia A., Mori G., 2010. *Biosensors & Bioelectronics*; 26, 2232-2236.

88. Tombelli S., Mascini M., Turner A.P.F., 2002. *Bioelectronics*; 17, 929-936.

89. Giannetto M., Umiltà E., Careri M., 2014. *Anal Chim Acta*; 806, 197-203.

90. Manfredi A., Giannetto M., Mattarozzi M., Mucchino C., Careri M., 2016. *Anal Bioanal Chem*; 408, 7289-7298.